# Bifurcation analysis and application for impulsive systems with delayed impulses

KEVIN E.M. CHURCH
*Department of Applied Mathematics, University of Waterloo, 200 University Avenue W, Waterloo, Ontario, N2L 3G1, Canada*
*k5church@uwaterloo.ca*

XINZHI LIU
*Department of Applied Mathematics, University of Waterloo, 200 University Avenue W, Waterloo, Ontario, N2L 3G1, Canada*
*xzliu@uwaterloo.ca*

*Electronic version of an article published in* International Journal of Bifurcation and Chaos*, Volume 27, Issue 12, November 2017, 1750186 [23 pages]. DOI: 10.1142/S0218127417501863,* 

In this article, we present a systematic approach to bifurcation analysis of impulsive systems with autonomous or periodic right-hand sides that may exhibit delayed impulse terms. Methods include Lyapunov-Schmidt reduction and center manifold reduction. Both methods are presented abstractly in the context of the stroboscopic map associated to a given impulsive system, and are illustrated by way of two in-depth examples: the analysis of a SIR model of disease transmission with seasonality and unevenly distributed moments of treatment, and a scalar logistic differential equation with a delayed census impulsive harvesting effort. It is proven that in some special cases, the logistic equation can exhibit a codimension 2 bifurcation at a 1:1 resonance point.

*Keywords*: Bifurcation theory, impulsive delay differential equations, SIR model, logistic equation

## 1. Introduction

Impulsive differential equations see applications in numerous fields where the systems of study exhibit rapid jumps in state. Such jumps may be intrinsic to the system, such as in the firing of a neuron in a biological neural network, or synthetic, such as the application of an insecticide or antibiotic treatment in a biological model. Arguably, one of the most common applications of the theory of impulsive differential equations arises in the latter case, where a continuous autonomous system is perturbed by impulses in an impulsive control setting. Specifically, there are many applications involving systems of the form

$$\dot{x} = F(x), \quad t \neq kT \tag{1}$$
$$\Delta x = G(x), \quad t = kT, \tag{2}$$

where (1) describes the continuous evolution of the system, and (2) the discontinuous impulsive control. We will call such a system an *impulsive system with autonomous right-hand side*; see [Bachar, Raimann & Kotanko, 2016; Church & Smith?, 2016; Rozins & Day, 2017; Xie et. al, 2017] for a few recent examples in mathematical biology. Such systems can be studied by exploiting their inherent periodicity properties.

Specifically, the study of local bifurcations of fixed points or periodic orbits of system (1)–(2) can be reduced to a problem in discrete time.

Consider the parameter-dependent system

$$\dot{x} = F(t, x, p), \quad t \neq \tau_k(p) \tag{3}$$
$$\Delta x = G_k(x, p), \quad t = \tau_k(p), \tag{4}$$

for parameter $p$ an element of a parameter space $\Pi$, where one has $\tau_{k+c}(p) = T(p) + \tau_k(p)$ for some $c > 0$ for all $p \in \Pi$, while $F(\cdot, x, p)$ is $T(p)$-periodic and $G_{k+c} = G_k$ for all $k$. If one defines the *stroboscopic map* $S : X \times \Pi \to X$ as a Poincaré map transversal to the surface $t = T(p)$ parameterized by the parameter $p$ in the periodic cylinder $X \times [0, T(p))$, then the stroboscopic map transforms the problem of identifying (parameter-dependent) periodic solutions of the piecewise-continuous system (3)–(4) with that of identifying (parameter-dependent) fixed points $x$ of the map $S$. The latter problem falls under the heading of bifurcations of fixed points or bifurcation theory of discrete-time systems, and there are numerous references devoted to this topic; for an introduction, see such elementary monographs as [Kuznetsov, 2004].

There is a very obvious difficulty with applying these techniques, however. The map $S$ is almost never explicitly available, since it is defined in terms of the solution of the (generally) nonlinear ordinary differential equation (3). The partial derivatives of $S$ at a given fixed point can be computed up to a given order by sequentially solving systems of linear inhomogeneous impulsive differential equations. This is the approach that is taken in the majority of the literature; see [Church & Smith?, 2016; Pang, Shen & Zhao, 2016; Xie et. al, 2017] for a few recent applications of these techniques to biological systems. However, the inherently cumbersome notation inevitably makes this process rather difficult in practice. Indeed, there has been to our knowledge no systematic outline of how the process should be completed. The goal of Section 2 and Section 3 is to remedy this problem by outlining how to perform an analysis of bifurcations at a nonhyperbolic equilibrium or periodic orbit of an impulsive systems with autonomous or periodic right-hand side.

Also of recent interest is the interaction between impulses and delays, such as in population dynamics, neural networks and synchronization [Xia, 2011; Liu & Wang, 2008; Zhou, Xiang & Liu, 2007]. Insofar as bifurcation theory of impulsive systems with delays is concerned, there is little in the way of established techniques, despite numerical investigations of particular impulsive systems with delays suggesting at traditional Hopf and period-doubling bifurcation patterns, among others [Yu et. al, 2010; Zhao et. al, 2012]. In Section 4, we briefly demonstrate that parameter-dependent systems of the form

$$\begin{aligned} \dot{x} &= F(t, x, p), && t \neq \tau_k(p) \\ \Delta x &= G_k(x, x(t - r_1(p)), \ldots, x(t - r_j(p)), p), && t = \tau_k(p), \end{aligned}$$

can be transformed into a finite set of equivalent impulsive differential equations without delays, for which the methods of Section 2 and Section 3 are applicable.

We conclude with two examples. Section 5 is an analysis of a transcritical bifurcation in the classical SIR model of disease transmission with unevenly spaced impulsive treatment. In Section 6, a scalar logistic equation with a census-delayed impulsive harvesting effort is considered, and a 1:1 resonance codimension two bifurcation is studied.

## 2. Stroboscopic map: elementary properties

The goal of this section will be to present a unified approach to bifurcation theory of periodic impulsive systems based on approximation of the stroboscopic (or Poincaré) map. One matter that we will consider that is absent from the literature is how to deal with equations where the moments of impulse or the period of the system depend on the parameter. In this section, our object of interest will be an impulsive system of the form

$$\dot{x} = f(t, x, \lambda), \quad t \neq \tau_k(\lambda) \tag{P1}$$
$$\Delta x = g_k(x, \lambda), \quad t = \tau_k(\lambda), \tag{P2}$$

where all functions appearing above are smooth and one has

$$g_{k+c} = g_k, \quad f(t, \cdot, \lambda) = f(t + T(\lambda), \cdot, \lambda), \quad \tau_{k+c}(\lambda) = \tau_k(\lambda) + T(\lambda). \tag{$P3$}$$

The number $T(\lambda)$ is the *period* of (P1)–($P3$) for parameter $\lambda$. Note we do not allow $c$ to depend on the parameter; bifurcation phenomena involving such dependences are inherently nonsmooth and will not be considered in this article.

### 2.1. *Nonautonomous processes*

For the impulsive differential equation (P1)–($P3$) , let the partial map

$$\phi : \mathbb{R} \times \mathbb{R} \times \Omega \times \Pi \to \Omega$$

denote the associated nonautonomous process, dependent on the parameter $\lambda \in \Pi$. That is, $\phi$ satisfies the following properties.

- $\phi(t, t, x, \lambda) = x$ for all $t \in \mathbb{R}, x \in \Omega$ and $\lambda \in \Pi$.
- $\phi(t, v, \phi(v, s, x, \lambda), \lambda) = \phi(t, s, x, \lambda)$ for all $s \leq v \leq t$ and $x \in \Omega$, $\lambda \in \Pi$.
- For each $s \in \mathbb{R}$, $x \in \Omega$ and $\lambda \in \Pi$, the function $t \mapsto \phi(t, s, x, \lambda)$ is defined on some $[s, \alpha)$ and is a solution of (P1)–(P2) .

In this article we take the convention that solutions are continuous from the left, as this seems to be the typical convention when dealing with finite-dimensional impulsive differential equations. It is known [Bainov & Simeonov, 1993] that if all functions defining (P1)–($P3$) are $k$ times continuously differentiable except possibly at times $t = \tau_k$ where they are continuous from the left with right limits, then $\phi$ is $k + 1$ times continuously differentiable in a neighborhood of $(t, s, x, \lambda)$, provided $t, s \notin \{\tau_k(\lambda)\}_{k \in \mathbb{Z}}$.

### 2.2. *Stroboscopic map*

An important construction based on the process $\phi$ is the stroboscopic map. To begin, assume the following additional hypotheses.

- All solutions of (P1)–($P3$) are defined indefinitely forward in time.
- $\tau_0(\lambda) = 0$ for all $\lambda \in \Pi$.
- (P1)–($P3$) is *formally* $C^k$; that is, $f$ and $D^k_{(x,\lambda)} f$ exist and are continuous, and $g_j$ is $C^k$ for each $j \in \mathbb{Z}$, and $\tau_j$ is $C^k$ for each $j \in \mathbb{Z}$. This will be abbreviated with the symbol $FC^k$.

The second condition can always be accomplished by a parameter-dependent change of time, and may always be assumed without loss of generality. Define the function $S : \Omega \times \Pi \to \Omega$ by

$$S(x, \lambda) = \phi(T(\lambda), 0, x, \lambda).$$

We call $S$ the *stroboscopic map for the impulsive differential equation* (P1)–($P3$) . We may occasionally abuse notation and identify a periodic solution $x^*$ with its value at time $t = 0$. For example, if $x^*$ is a periodic solution, we might write $S(x^*, \lambda) := S(x^*(0), \lambda)$. Fundamental to our methodology is that the stroboscopic map is as smooth as the impulsive differential equation and preserves stability properties.

**Proposition 1.** *The stroboscopic map $S : \Omega \times \Pi \to \Omega$ is $k$ times continuously differentiable.*

**Proposition 2.** *Let $x^*$ be a periodic orbit for* (P1)–($P3$) *with parameter $\lambda$. Then, $x^*(0)$ is a uniformly stable (resp. uniformly asymptotically stable) fixed point of the discrete-time dynamical system $x_{n+1} = S(x_n, \lambda)$ if and only if the periodic orbit $x^*$ is uniformly stable (resp. uniformly asymptotically stable) as a periodic orbit of* (P1)–($P3$).

### 2.3. *Derivatives of the stroboscopic map*

The partial derivatives of the stroboscopic map at a given point are related to a hierarchy of impulsive differential equations. Beginning with first-order terms, the system is linear, and the order $n+1$ terms can be computed by solving a linear system that depends nonlinearly on the order $n$ terms. For derivatives of higher order than one in the parameter, the equations become intractable, in the sense that stating them in full generality is of little use. First, we will include a result that follows directly from a theorem from the monograph of Bainov and Simeonov [Bainov & Simeonov, 1993].

**Theorem 1** [Theorem 2.10, [Bainov & Simeonov, 1993]]. *Consider the solution map $x(t;\cdot,\cdot,\cdot):\mathbb{R}\times\Omega\times\Pi\to\Omega$ of the $FC^k$ system* (P1)–(P2). *Denote $x(t)=x(t;t_0,x_0,\lambda_0)$, $u=\frac{\partial x}{\partial x_0}(t;t_0,x_0,\lambda_0)$, $v=\frac{\partial x}{\partial\lambda}(t;t_0,x_0,\lambda_0)$. If $t_0\notin\{\tau_k(\lambda):k\in\mathbb{Z}\}$, then $u$ and $v$ satisfy the following initial-value problems:*

$$\begin{aligned}
\dot u &= D^x f(t,x(t),\lambda_0)u, && t\neq\tau_k(\lambda_0)\\
\Delta u &= D^x g_k u, && t=\tau_k(\lambda_0)\\
\dot v &= D^x f(t,x(t),\lambda_0)v + D^\lambda f(t,x(t),\lambda_0), && t\neq\tau_k(\lambda_0)\\
\Delta v &= D^x g_k v + D^\lambda g_k - [f^+ - f - D^x g_k f]D^\lambda\tau_k(\lambda_0), && t=\tau_k(\lambda_0)\\
u(0) &= I_{n\times n},\\
v(0) &= 0,
\end{aligned}$$

*where $D^x g_k$ and $D^\lambda g_k$ are evaluated at $(x(\tau_k),\lambda_0)$, and $f=f(\tau_k,x(\tau_k),\lambda_0)$, $f^+=f(\tau_k(\lambda_0),x(\tau_k^+),\lambda_0)$.*

#### 2.3.1. *One derivative in the parameter*

Due to the continuity of the map $t_0\mapsto x(t;t_0,x_0,\lambda_0)$ from the left, the requirement that $t_0\notin\{\tau_k(\lambda):k\in\mathbb{Z}\}$ of Theorem 1 can be dropped. This fact is the reason we are able to obtain the following theorem.

**Theorem 2.** *Let $x^*$ be a $T(\lambda^*)$-periodic solution of the $FC^k$ system* (P1)–(P3) *for parameter $\lambda^*$. Let $\mathbf{m}=(\vec{x}^\alpha,\vec{\lambda}^\beta)=(x_1^{\alpha_1},\dots,x_n^{\alpha_n},\lambda_1^{\beta_1},\dots,\lambda_m^{\beta_m})$ denote a multiindex with $|\beta|\in\{0,1\}$ and $|\mathbf{m}|\le k$. Then, one has*

$$\partial^{\vec{x}^\alpha}S(x^*,\lambda^*)=\partial^{\vec{x}^\alpha}\phi(T(\lambda^*),0,x^*,\lambda^*), \tag{5}$$

$$\partial^{\vec{x}^\alpha\lambda_i}S(x^*,\lambda^*)=\partial^{\vec{x}^\alpha}f(T(\lambda^*),\phi(T,0,x,\lambda^*),\lambda^*)\Big|_{x=x^*}\partial^{\lambda_i}T(\lambda^*)+\lim_{t\to T^-}\partial^{\vec{x}^\alpha\lambda_i}\phi(t,0,x^*,\lambda^*) \tag{6}$$

*and the function $v^{\mathbf{m}}(t)=\partial^{\mathbf{m}}\phi(t,0,x^*,\lambda^*)$ is differentiable at all times $t\neq\tau_k(\lambda)$ and satisfies the impulsive differential equation*

$$\dot v^{\mathbf{m}}=Df(t,x^*,\lambda^*)v^{\mathbf{m}}+F_{\mathbf{m}}(x^*,\lambda^*,v^{\mathbf{j}}:|\mathbf{j}|<|\mathbf{m}|),\quad t\neq\tau_k(\lambda^*) \tag{7}$$

$$\Delta v^{\mathbf{m}}=Dg_k(x^*,\lambda^*)v^{\mathbf{m}}+G_{\mathbf{m}}(x^*,\lambda^*,v^{\mathbf{j}}:|\mathbf{j}|<|\mathbf{m}|),\quad t=\tau_k(\lambda^*) \tag{8}$$

$$v(0)=\begin{cases}e_j,\ \mathbf{m}=x_j\\ 0\quad otherwise,\end{cases} \tag{9}$$

*for some (generally) nonlinear functions $F_{\mathbf{m}}$ and $G_{\mathbf{m}}$.*

*Proof.* The correctness of the form of equation (7)–(8) follows by an inductive argument on the order of the multiindex $\mathbf{m}$, based on Theorem 1. To prove (5) apply Proposition 1. For (6), write

$$S_\epsilon(x,\lambda)=C(T(\lambda)-\epsilon,\tau_{c-1}(\lambda),\phi(\tau_{c-1}(\lambda)^+,0,x,\lambda))$$

where $C$ denotes the continuous process associated to (P1). Then, $D^{\mathbf{m}}S(x,\lambda)=\lim_{\epsilon\to0^+}D^{\mathbf{m}}S_\epsilon(x,\lambda)$. Carefully taking appropriate partial derivatives and the limit produces the desired result. ■

*Remark 2.1.* The term $\partial^{\vec{x}^\alpha} f(T, \phi(T,0,x,\lambda^*),\lambda^*)|_{x=x^*}$ with $T = T(\lambda^*)$ must be computed by $|\alpha|$ iterations of the chain rule in conjunction with the Leibniz law. For example, we have

$$\begin{aligned}\partial^{x_1x_2x_3} f(T,\phi(T,0,x,\lambda^*)) &= \partial^{x_1x_2}[Df(T,0,\phi,\lambda^*)\partial^{x_3}\phi]\\ &= \partial^{x_1}\left[D^2f(T,0,\phi,\lambda^*)[\partial^{x_2}\phi,\partial^{x_3}\phi] + Df(T,0,\phi,\lambda)\partial^{x_2x_3}\phi\right]\\ &= D^3f(T,0,\phi,\lambda^*)[\partial^{x_3}\phi,\partial^{x_2}\phi,\partial^{x_1}\phi] + D^2f(T,0,\phi,\lambda^*)[\partial^{x_1x_2}\phi,\partial^{x_3}\phi]\\ &\quad + D^2f(T,0,\phi,\lambda^*)[\partial^{x_2}\phi,\partial^{x_3x_1}\phi] + D^2f(T,0,\phi,\lambda^*)[\partial^{x_1}\phi,\partial^{x_2x_3}\phi]\\ &\quad + Df(T,0,\phi,\lambda^*)\partial^{x_1x_2x_3}\phi.\end{aligned}$$

The final correct result for $\partial^{\vec{x}^\alpha} f(T,\phi(T,0,x,\lambda^*),\lambda^*)|_{x=x^*}$ is then obtained by evaluating $\phi = \phi(T,0,x,\lambda)$ and all its partial derivatives appearing above at $x = x^*$. If $S(x^*,\lambda^*) = x^*$, as is the case when one is considering bifurcation of a periodic solution $t \mapsto \phi(t,0,x^*,\lambda^*)$, then the result is precisely

$$\begin{aligned}\partial^{x_1x_2x_3} f(T,\phi(T,0,x,\lambda^*))|_{x=x^*} &= D^3f(T,0,x^*,\lambda^*)[v^{x_3},v^{x_2},v^{x_1}] + D^2f(T,0,x^*,\lambda^*)[v^{x_1x_2},v^{x_3}]\\ &\quad + D^2f(T,0,x^*,\lambda^*)[v^{x_2},v^{x_3x_1}] + D^2f(T,0,x^*,\lambda^*)[v^{x_1},v^{x_2x_3}]\\ &\quad + Df(T,0,x^*,\lambda^*)v^{x_1x_2x_3},\end{aligned}$$

where each $v^{\vec{x}^\alpha}$ is evaluated at time $t = T(\lambda)$. Similarly,

$$\begin{aligned}\partial^{x_1x_2} f(T,\phi(T,0,x,\lambda^*))|_{x=x^*} &= D^2f(T,0,x^*,\lambda^*)[v^{x_1},v^{x_2}] + Df(T,0,x^*,\lambda^*)v^{x_1x_2},\\ \partial^{x_1} f(T,\phi(T,0,x,\lambda^*))|_{x=x^*} &= Df(T,0,x^*,\lambda^*)v^{x_1}.\end{aligned}$$

The differential equations of Theorem 2 are available explicitly in the form of Table 1. This table together with equations (5)–(6) can be readily referenced to compute the partial derivatives of the stroboscopic map up to order three in state and order one in the parameter. The table includes terms of the form $D^kh(t,x^*,\lambda^*)[x^1,x^2,\ldots,x^m]$ for $h$ a smooth function, $t \in \mathbb{R}$, $\lambda^* \in \Pi$ and $x^*, x^i \in \mathbb{R}^n$. The action of the symmetric $k$-linear map $D^kh(t,x^*,\lambda^*)$ on the tuple $[x^1,\ldots,x^k]$ can be computed according to [Loomis & Sternberg, 1968] as

$$D^kh[x^1,\ldots,x^k] = \sum_{i_1,\ldots,i_k=1}^{n} x^1_{i_1}\cdots x^k_{i_k}\frac{\partial^k h}{\partial x_{i_1}\cdots\partial_{x_{i_k}}}(t,x^*,\lambda^*). \tag{10}$$

### 2.3.2. *Several derivatives in the parameter*

When the period $T$ and impulse times $\tau_k$ are independent of the parameter, higher-order derivatives of the stroboscopic map involving the parameter can be obtained by formally differentiating the appropriate differential equations of Table 1 sufficiently many times, and solving the associated linear impulsive equations. When the period and/or impulse times depend nontrivially on the parameter, this approach does not work, and one must be careful in determining appropriate impulsive differential equations that generate the derivatives.

For example, suppose one wishes to calculate $\partial^{\lambda^2} S$ for scalar parameter $\lambda$, with state vector $x \in \mathbb{R}^n$. By a similar argument to the proof of Theorem 2, it follows that

$$\partial^{\lambda^2} S = \partial^t f\cdot(\partial^\lambda T)^2 + Df\cdot\partial^\lambda\phi\cdot\partial^\lambda T + \partial^\lambda f\cdot\partial^\lambda T + \lim_{t\to T^-}\partial^{\lambda\lambda}\phi,$$

where $f$ and $Df$ are evaluated at $(T(\lambda^*),\phi,\lambda^*)$, all instances of $\phi$ are evaluated at $(T(\lambda^*),0,x^*,\lambda^*)$, and $T$ is evaluated at $\lambda^*$. The function $v^{\lambda\lambda}(t) = \partial^{\lambda\lambda}\phi(t,0,x^*,\lambda^*)$ satisfies a particular impulsive differential

Table 1. Explicit form of differential equations described in Theorem 2 for order at most three, with at most one derivative with respect to the parameter. All function evaluations have been suppressed; $f$, $g_k$ and all differentials are evaluated at $(t, x^*(t), \lambda^*)$ in the continuous time-derivative equations $(\dot{v}^{\mathbf{m}})$ and at $(\tau_k(\lambda^*), x^*(\tau_k(\lambda^*), \lambda^*)$ in the discrete difference $(\Delta v^{\mathbf{m}})$ equations, except for where otherwise noted. Also, $f^+$ indicates that all time arguments are evaluated in the limit as $t \to \tau_k^+$. The $k$th-order differentials $D^k h[x^1, x^2, \ldots, x^k]$ can be computed as per equation (10). Note that, if $x^*(t)$ is an equilibrium point, then one has $f^+ = f = 0$, $Df^+ = Df$, and many terms in the $\Delta v^{x\lambda_j}$ equations will cancel.

| | |
|---|---|
| $x_i$ | $\begin{aligned} \dot{v}^{x_i} &= D^x f \cdot v^{x_i}, \\ \Delta v^{x_i} &= D^x g_k \cdot v^{x_i}, \\ v^{x_i}(0) &= e_i. \end{aligned}$ |
| $\lambda_i$ | $\begin{aligned} \dot{v}^{\lambda_i} &= D^x f \cdot v^{\lambda_i} + D^{\lambda_i} f\cdot, \\ \Delta v^{\lambda_i} &= D^x g_k \cdot v^{\lambda_i} + D^{\lambda_i} g_k - [f^+ - f - D^x g_k \cdot f] D^{\lambda_i} \tau_k(\lambda^*) \\ v^{\lambda_i}(0) &= 0 \end{aligned}$ |
| $x_i x_j$ | $\begin{aligned} \dot{v}^{x_i x_j} &= D^x f \cdot v^{x_i x_j} + D^{xx} f \cdot [v^{x_i}, v^{x_j}], \\ \Delta v^{x_i x_j} &= D^x g_k \cdot v^{x_i x_j} + D^{xx} g_k \cdot [v^{x_i}, v^{x_j}] \\ v^{x_i x_j}(0) &= 0 \end{aligned}$ |
| $x_i \lambda_j$ | $\begin{aligned} \dot{v}^{x_i \lambda_j} &= D^x f \cdot v^{x_i \lambda_j} + D^{xx} f \cdot [v^{x_i}, v^{\lambda_j}] + D^x (D^{\lambda_j} f) \cdot v^{x_i}, \\ \Delta v^{x_i \lambda_j} &= D^x g_k \cdot v^{x_i \lambda_j} + D^{xx} g_k \cdot [v^{x_i}, v^{\lambda_j}] + D^x (D^{\lambda_j} g_k) \cdot v^{x_i} \\ &\quad - [D^x f^+ \cdot v^{x_i}(\tau_k^+) - D^x f \cdot v^{x_i} - D^{xx} g_k \cdot [f, v^{x_i}] - D^x g_k \cdot D^x f \cdot v^{x_i}] D^{\lambda_j} \tau_k(\lambda^*) \\ v^{x_i \lambda_j}(0) &= 0 \end{aligned}$ |
| $x_i x_j x_m$ | $\begin{aligned} \dot{v}^{x_i x_j x_m} &= D^x f \cdot v^{x_i x_j x_m} + D^{xx} f \cdot [v^{x_i}, v^{x_j x_m}] + D^{xx} f \cdot [v^{x_j}, v^{x_i x_m}] + D^{xx} f \cdot [v^{x_m}, v^{x_i x_j}] \\ &\quad + D^{xxx} f \cdot [v^{x_i}, v^{x_j}, v^{x_m}] \\ \Delta v^{x_i x_j x_m} &= D^x g_k \cdot v^{x_i x_j x_m} + D^{xx} g_k \cdot [v^{x_i}, v^{x_j x_m}] + D^{xx} g_k \cdot [v^{x_j}, v^{x_i x_m}] + D^{xx} g_k \cdot [v^{x_m}, v^{x_i x_j}] \\ &\quad + D^{xxx} g_k \cdot [v^{x_i}, v^{x_j}, v^{x_m}] \\ v^{x_i x_j x_m}(0) &= 0 \end{aligned}$ |
| $x_j x_j \lambda_m$ | $\begin{aligned} \dot{v}^{x_i x_j \lambda_m} &= D^x f \cdot v^{x_j x_j \lambda_m} + D^{xx} f \cdot [v^{x_i}, v^{x_j \lambda_m}] + D^{xx} f \cdot [v^{x_j}, v^{x_i \lambda_m}] + D^{xx} f \cdot [v^{\lambda_m}, v^{x_i x_j}] \\ &\quad + D^{xxx} f \cdot [v^{x_i}, v^{x_j}, v^{\lambda_m}] + D^{xx} (D^{\lambda_m} f) \cdot [v^{x_i}, v^{x_j}] + D^x (D^{\lambda_m} f) \cdot v^{x_i x_j} \\ \Delta v^{x_i x_j \lambda_m} &= D^x g_k \cdot v^{x_i x_j \lambda_m} + D^{xx} g_k \cdot [v^{x_i}, v^{x_j \lambda_m}] + D^{xx} g_k \cdot [v^{x_j}, v^{x_i \lambda_m}] + D^{xx} g_k \cdot [v^{\lambda_m}, v^{x_i x_j}] \\ &\quad + D^{xxx} g_k \cdot [v^{x_i}, v^{x_j}, v^{\lambda_m}] + D^{xx} (D^{\lambda_m} g_k) \cdot [v^{x_i}, v^{x_j}] + D^x (D^{\lambda_m} g_k) \cdot v^{x_i x_j} \\ &\quad - \Big( D^{xx} f^+ [v^{x_i}(\tau_k^+), v^{x_j}(\tau_k^+)] + D^x f^+ \cdot v^{x_i x_j}(\tau_k^+) - D^{xx} f \cdot [v^{x_i}, v^{x_j}] - D^x f \cdot v^{x_i x_j} \\ &\quad - D^{xxx} g_k \cdot [f, v^{x_i}, v^{x_j}] - D^{xx} g_k \cdot [D^x f \cdot v^{x_i}, v^{x_j}] - D^{xx} g_k \cdot [D^x f \cdot v^{x_j}, v^{x_i}] \\ &\quad - D^{xx} g_k \cdot [f, v^{x_i x_j}] - D^x g_k \cdot D^{xx} f \cdot [v^{x_i}, v^{x_j}] \Big) D^{\lambda_m} \tau_k(\lambda^*) \\ v^{x_i x_j \lambda_m}(0) &= 0 \end{aligned}$ |

equation. To obtain this equation, one could apply row two of Table 1 to itself. The continuous part is

$$\begin{aligned} \dot{v}^{\lambda\lambda} &= D^x [D^x f \cdot v^\lambda + D^\lambda f] \cdot v^\lambda + D^\lambda [D^x f \cdot v^\lambda + D^\lambda f] \\ &= \Big( D^{xx} f \cdot [D^x \phi \cdot v^\lambda, v^\lambda] + D^x f \cdot [D^x v^\lambda \cdot v^\lambda] + D^{x\lambda} f \cdot [D^x \phi \cdot v^\lambda] \Big) \\ &\quad + \Big( D^{xx} f \cdot [D^\lambda \phi, v^\lambda] + D^{\lambda x} f \cdot v^\lambda + D^x f \cdot D^\lambda v^\lambda + D^{\lambda x} f \cdot D^\lambda \phi + D^{\lambda\lambda} f \Big) \\ &= D^{xx} f \cdot [v^x v^\lambda, v^\lambda] + D^{xx} f \cdot [v^\lambda, v^\lambda] + D^{x\lambda} f \cdot v^x v^\lambda + D^{\lambda x} f \cdot v^\lambda + D^{\lambda\lambda} f + D^x f \cdot v^{x\lambda} v^\lambda + D^x f \cdot v^{\lambda\lambda}. \end{aligned}$$

The impulsive part is much more complicated, and we do not provide it in its entirety here. Suffice it to say, without expanding fully, it is given by

$$\Delta v^{\lambda\lambda} = D^x (v^\lambda) \cdot v^\lambda + D^\lambda (\Delta v^\lambda) - [\dot{v}^\lambda(\tau_k^+) - \dot{v}^\lambda(\tau_k) - D^x (\Delta v^\lambda) \cdot \dot{v}^\lambda(\tau_k)] D^\lambda \tau_k(\lambda^*).$$

The following Lemma will surely provide some use in those cases where the period of the system and impulse times do not depend on the parameter. The proof is obvious and is omitted.

**Lemma 1.** *Suppose the sequence of impulse times ($\tau_k$) and the period ($T$) do not depend on $\lambda$. Then, the stroboscopic map associated to* (P1)–(P2) *satisfies $\partial^\alpha S(x^*,\lambda^*) = \lim_{t\to T^-}\partial^\alpha\phi(t,0,x^*,\lambda^*)$ for all multi-indices $\alpha$ such that $t\mapsto\partial^\alpha\phi(t,0,x^*,\lambda^*)$ is $FC^0$.*

## 3. Reduction methods for impulsive systems

In Section 2 we introduced the stroboscopic map associated to a periodic impulsive differential equation and proved that its derivatives at a given reference solution or equilibrium point can be computed by solving tiered systems of linear impulsive differential equations (Theorem 2). In this section, we will outline two methods frequently used in the literature to analyze bifurcations of impulsive systems with autonomous or periodic right-hand sides. Explicit examples will be provided to demonstrate the method as applied to traditional models in mathematical biology. The two methods that will be outlined are *Lyapunov-Schmidt reduction* and *center manifold reduction*. These techniques yield similar information, although each has its advantages and disadvantages. Broadly speaking, both methods reduce the dimension of the nonlinear equation that must be studied to the number of critical eigenvalues – that is, the number of eigenvalues of $D^xS(x^*,\lambda^*)$ that have unit modulus.

### 3.1. *Lyapunov-Schmidt reduction*

Let $S:\mathbb{R}^n\times\Lambda\to\mathbb{R}^n$ denote the stroboscopic map of the system (P1)–(P2), where $S(x^*,\lambda^*)=x^*$, so that $x^*$ corresponds to a $T(\lambda^*)$-periodic orbit (or equilibrium) of the system. Let the equilibrium be nonhyperbolic; that is, there is at least one eigenvalue $\mu\in\sigma(D^XS(x^*,\lambda^*))$ with $|\mu|=1$. Let this eigenvalue satisfy $\mu^k=1$; it follows that 1 is an eigenvalue of $D^xS^k(x^*,\lambda^*)$. To be clear, $S^k$ denotes $k$-fold composition in the variable $x$;

$$S^k(x,\lambda)=S(\cdot,\lambda)\circ\cdots\circ S(\cdot,\lambda)\circ S(x,\lambda)$$

where there are $k$ compositions. It follows that $\mu=e^{i2\pi\theta}$ and $\theta$ is rational, so this approach cannot be used to study Neimark-Sacker bifurcations with irrational $\theta$.

Define the function $N:\mathbb{R}^n\times\Lambda\to\mathbb{R}^n$ by $N(x,\lambda)=S^k(x+x^*,\lambda+\lambda^*)-(x+x^*)$. Zeroes $(y,\mu)$ of $N$ satisfy

$$N(y,\mu)=0=S^k(y+x^*,\mu+\lambda^*)-(y+x^*)\Rightarrow S^k(y+x^*,\mu+\lambda^*)=y+x^*,$$

and so uniquely determine fixed points of $S^k$ and vice versa. This can be though of as a linear change of coordinates:

$$x=y+x^*,\qquad \lambda=\mu+\lambda^*.$$

Notice that, for a multiindex $\mathbf{m}=(x_1^{\alpha_1},\dots,x_n^{\alpha_n},\lambda_1^{\beta_1},\dots,\lambda_m^{\beta_m})$ with $|\alpha|\geq 2$ or $|\beta|\geq 1$, we have $D^{\mathbf{m}}N(0,0)=D^{\mathbf{m}}S^k(x^*,\lambda^*)$. Therefore, each partial derivative of $N$ can in principle be calculated by first expressing $S(x,\lambda)$ in a Taylor series expansion near $(x^*,\lambda^*)$; if $k=1$, the order $\alpha$ terms coincide with those of $N(x,\lambda)$. Computing $D^\alpha S(x^*,\lambda^*)$ can be accomplished by Theorem 2 and application of Table 1, so we may assume that

$$N(x,\lambda)=\sum_{0<|\mathbf{m}|\leq k}\frac{1}{\mathbf{m}!}D^{\mathbf{m}}N(0,\lambda^*)\cdot(x,\lambda)^{\mathbf{m}}+O((x,\lambda)^{k+1}),$$

where $(x,\lambda)^{\mathbf{m}}=x_1^{\alpha_1}\cdots x_n^{\alpha_n}\lambda_1^{\beta_1}\cdots\lambda_m^{\beta_m}$.

The rest of the reduction procedure follows by standard results of functional analysis, but we will collect the main ideas here. By definition, $\mathcal{N}:=D^xN(0,0)$ has at least one zero eigenvalue and the kernel of $\mathcal{N}$, denoted $\ker(\mathcal{N})$, is at least one-dimensional. Let $B=\{v_1,\dots,v_{n_c}\}$ be an orthogonal basis of $\ker(\mathcal{N})$, and let $y\in\mathbb{R}^n$ be written in the direct sum decomposition $y=y_0+\hat{y}$ with $y_0\in\ker(\mathcal{N})$ and $\hat{y}\in\ker(\mathcal{N})^\perp$;

one has $y_0 = \text{proj}_B y$ and $\hat{y} = y - y_0$. Let $P$ be a projection onto the range $r(\mathcal{N})$ of $\mathcal{N}$ (that is, $P$ is a linear operator with $P^2 = P$ whose range is $r(\mathcal{N})$).

Because $P$ is a projection operator, we see that $(x, \lambda)$ satisfies the equation $N(x, \lambda) = 0$ if and only if both $PN(x, \lambda) = 0$ and $(I - P)N(x, \lambda) = 0$. The range of $PN : \mathbb{R}^n \times \Lambda \to \mathbb{R}^n$ is a subset of $r(\mathcal{N})$. In particular, due to the direct sum decomposition of $\mathbb{R}^n$ by the kernel of $\mathcal{N}$, we can instead write

$$PN : (\ker(\mathcal{N}) \times \ker(\mathcal{N})^{\perp}) \times \Lambda \to r(\mathcal{N}),$$

and consider the solvability of the equation $N_1(y_0, \hat{y}, \lambda) := PN(y_0 + \hat{y}, \lambda) = 0$. Clearly $N_1$ is $C^1$, and we have that $D^{\hat{y}} N_1(0, 0, 0) = P\mathcal{N} = \mathcal{N}$. Since $\dim \ker(N)^{\perp} = \dim r(\mathcal{N})$ and $\mathcal{N}$ is onto its range, it follows that $y \mapsto D^{\hat{y}} N_2(0, 0, 0)y$ is an isomorphism, and is therefore invertible. By the implicit function theorem, there exists a unique function $\hat{y} = \hat{y}(y_0, \lambda)$ with the property that

$$PN(y_0 + \hat{y}(y_0, \lambda), \lambda) = 0$$

for all $(y_0, \lambda)$ sufficiently close to $(0, 0)$. Therefore, our task has been simplified to solving the equation $(I - P)N(y_0 + \hat{y}(y_0, \lambda), \lambda) = 0$ near $(y_0, \lambda) = (0, 0)$. Our goal will be to identify all possible branches of solutions $y_0 = y_0(\lambda)$ that satisfy the *bifurcation equation*

$$N_2(y_0, \lambda) := (I - P)N(y_0(\lambda) + \hat{y}(y_0(\lambda), \lambda), \lambda) = 0. \tag{11}$$

The family of bifurcating $kT(\lambda)$-periodic solutions of the original impulsive differential equation will then be determined by

$$y^*(\lambda) \in y_0(\lambda) + \hat{y}(y_0(\lambda), \lambda), \tag{12}$$

for $|\lambda|$ small, where we have written set inclusion because $\lambda \mapsto y_0(\lambda)$ may be multivalued. Inverting the change of variables, we can alternatively write

$$x^*(\lambda) \in x^* + y_0(\lambda - \lambda^*) + \hat{y}(y_0(\lambda - \lambda^*), \lambda - \lambda^*) \tag{13}$$

for $|\lambda - \lambda^*|$ small.

### 3.2. *Center manifold reduction*

Center manifold reduction is a method of reducing the number of equations that must be studied to determine the structure of bifurcations in a system of ordinary differential equations or a discrete-time map. It is a dynamic method as opposed to a static method, such as Lyapunov-Schmidt reduction, since the dynamics of the underlying system are preserved by the reduction, and therefore yields stability information directly, making it more powerful than Lyapunov-Schmidt reduction. For additional information on center manifold reduction, see Kuznetsov [Kuznetsov, 2004].

Let $S(x, \lambda)$ be the stroboscopic map for the system (P1)–(P2), and let $S^k(x^*, \lambda^*) = x^*$; that is, $x^*$ corresponds to a $kT(\lambda^*)$-periodic solution of (P1)–(P2) for parameter $\lambda^*$. Let the periodic solution be nonhyperbolic. More precisely, let $D^x S^k(x^*, \lambda^*)$ have $n_c = n - n_{su} \geq 1$ eigenvalues on the complex unit circle.

We will need to define a translated stroboscopic map. Define $U(x, \lambda) = S(x + x^*, \lambda + \lambda^*) - x^*$. The parameter-augmented system

$$\begin{pmatrix} x_{n+1} \\ \lambda_{n+1} \end{pmatrix} = \mathbf{U}(x_n, \lambda_n) := \begin{pmatrix} U^k(x_n, \lambda_n) \\ \lambda_n \end{pmatrix}$$

has the fixed point $(0, 0)$ and $D\mathbf{U}(0, 0)$ has $n_c + 1$ eigenvalues on the unit circle. Using Theorem 2, one can express $\mathbf{U}$ as a Taylor expansion up to order $\ell$ in $(x, \lambda)$ near $(0, 0)$. This is typically accomplished by computing $D^\alpha S(x^*, \lambda^*)$ for various multiindices $\alpha$, and then using the chain rule numerous times to obtain $D^{\mathbf{m}} U^k(0, 0)$. Thus, one considers the problem

$$\begin{aligned} x_{n+1} &= \sum_{0 < |\mathbf{m}| \leq \ell} \frac{1}{\mathbf{m}!} D^{\mathbf{m}} U^k(0, 0) \cdot (x, \lambda)^{\mathbf{m}} + O((x, \lambda)^{\ell+1}) \\ \lambda_{n+1} &= \lambda_n, \end{aligned} \tag{14}$$

for multiindices $\mathbf{m} = (x^{\mathbf{m}_x}, \lambda^{\mathbf{m}_\lambda})$.

To perform the reduction, one now performs the typical center manifold reduction to the system (14). The first step is to obtain the real Jordan decomposition $DU^k(0,0) = PJP^{-1}$ where $J = \operatorname{diag}(E, C) \in \mathbb{R}^{n\times n}$ is block diagonal, $E$ is $(n-n_c)\times(n-n_c)$ has no eigenvalues on the unit circle and $C$ is $n_c \times n_c$ and has all its eigenvalues on the unit circle. The change of variables $x = Jy$ transforms the above system into

$$\begin{aligned} y_{n+1} &= Jy + P^{-1} \sum_{1<|\mathbf{m}|\le \ell} \frac{1}{\mathbf{m}!} D^{\mathbf{m}} U^k(0,0)(Py,\lambda)^{\mathbf{m}} + O((y_n,\lambda_n)^{\ell+1}) \\ \lambda_{n+1} &= \lambda_n. \end{aligned} \tag{15}$$

By writing $y = [\, w \; z\,]^T$ with $w \in \mathbb{R}^{n-n_c}$ and $z \in \mathbb{R}^{n_c}$, the above system can be equivalently written

$$w_{n+1} = Ew_n + F_1(w_n, z_n, \lambda_n) + O((w_n, z_n, \lambda_n)^{\ell+1}) \tag{16}$$

$$z_{n+1} = Cz_n + F_2(w_n, z_n, \lambda_n) + O((w_n, z_n, \lambda_n)^{\ell+1}) \tag{17}$$

$$\lambda_{n+1} = \lambda_{n+1}, \tag{18}$$

where $F = [\, F_1 \; F_2\,]^T$ is the terms of degree 2 through $\ell$ of (15). The Center Manifold Theorem then implies that there exists a function $w = h(z,\lambda)$ that is invariant under (16)–(18) and tangent to the linearized center subspace. By the invariance and tangency conditions, the function $w$ must satisfy the functional equation

$$\begin{aligned} Eh(z,\lambda) + F_1(h(z,\lambda), z, \lambda) &= h(Cz + F_2(h(z,\lambda), z, \lambda), \lambda) + O((w,z,\lambda)^{\ell+1}), \\ Dh(0,0) &= 0. \end{aligned} \tag{19}$$

By classical results of bifurcation theory for maps, with an expansion $h(z,\lambda) = h_\ell(z,\lambda) + O((z,\lambda)^{\ell+1})$, the transformed system (16)–(18) (and, by inverting the change of variables $x = Py$, the original iterated parameter-augmented system (14)) is locally topoogically conjugate near the origin to the system

$$\begin{aligned} w_{n+1} &= Ew_n + O^{\ell+1} \\ z_{n+1} &= Cz_n + F_2(h_\ell(z_n,\lambda_n), z_n, \lambda_n) + O^{\ell+1} \\ \lambda_{n+1} &= \lambda_n. \end{aligned} \tag{20}$$

Since the equations are decoupled and the first one (for $w$) is hyperbolic, bifurcations can be studied by considering only the equation (20), which is $n_c$-dimensional, and defines the nonhyperbolic part. In general, one must use of the normal form theory for maps to analyze the nonhyperbolic part and classify the type of bifurcation. One may consult such references as [Kuznetsov, 2004; Wiggins, 2003] for additional details.

## 4. Elimination of delay from a class of impulsive delay differential equations

Consider now the $n$-dimensional impulsive delay differential equation depending on a parameter $p \in \Pi$,

$$\dot{x} = F(t, x, p), \qquad t \neq \tau_k(p) \tag{21}$$

$$\Delta x = G_k(x, x(t - r_1(p)), \ldots, x(t - r_j(p)), p), \quad t = \tau_k(p), \tag{22}$$

where as before, we assume the periodicity conditions $F(t + T(p), \cdot, p) = F(t, \cdot, p)$, $\tau_{k+c}(p) = \tau_k(p) + T(p)$ and $G_{k+c} = G_k$ for all $k \in \mathbb{Z}$ and $t \in \mathbb{R}$. Also, we will take the convention here that solutions of the impulsive delay differential equation above are continuous from the left. This means that the impulse condition (22) is equivalent to

$$x(\tau_k^+) = x(\tau_k) + G_k(x(\tau_k), x(\tau_k - r_1), \ldots, x(\tau_k - r_j)),$$

where we have suppressed the parameter for compactness of notation. Note that this is in contrast to the majority of the literature on impulsive delay differential equations, where the convention is to define solutions as being continuous from the right. It turns out that the choice of solution formalism – that is, left-continuous or right-continuous – does have an impact on how the system (21)–(22) is transformed into a finite-dimensional problem. However, we will not elaborate on the right-continuous case here.

Assume the impulses and delays satisfy the following ordering property: for all $i \in \{1, \ldots, j\}$ and all $k \in \{0, \ldots, c-1\}$, the inequality

$$\tau_k(p) + r_i(p) < \tau_{k+1}(p) \tag{23}$$

is satisfied. Introduce piecewise-constant variables $y_i$ by the relation

$$y_i(t) = \big\{ x(\tau_k - r_i),\, t \in (\tau_k - r_i, \tau_{k+1} - r_i],$$

where we suppress the parameter $p$ for clarity. Under the ordering property (23), each $y_i$ is well-defined and continuous from the left. System (21)–(22) is equivalent to the following $(n + jn)$-dimensional impulsive systems without delays.

$$\dot{x} = F(t, x, p), \qquad t \notin \{\tau_k(p), \tau_k(p) - r_i(p)\}_{i=1,\ldots,j} \tag{24}$$
$$\dot{y}_i = 0, \qquad t \notin \{\tau_k(p), \tau_k(p) - r_i(p)\}_{i=1,\ldots,j} \tag{25}$$
$$\Delta x = G_k(x, y_1, \ldots, y_j, p), \quad t = \tau_k(p) \tag{26}$$
$$\Delta y_i = x - y_i, \qquad t = \tau_k(p) - r_i(p). \tag{27}$$

Bifurcations can be studied in system (24)–(27) using the finite-dimensional methods described in Section 3. The $y_i$ states can then be ignored to obtain analogous bifurcation results for the original system (21)–(22). The period of the system (24)–(27) is $T(p)$, but the number of impulses per period is $n(p) = c + jc$.

When the ordering property (23) is violated non-strictly — that is, $\tau_k(p) + r_i(p) \leq \tau_{k+1}(p)$ for all pairs $(i, k)$ — the above method proceeds without a great deal of modification, and one obtains a finite-dimensional system of impulsive differential equations that is equivalent to (21)–(22). However, in such instances, one cannot directly consider $p$ as a bifurcation parameter because the stroboscopic map is generally non-smooth at such parameters where the ordering property fails.

For instance, suppose at scalar parameter $p = p^*$, there is at least one pair $(i, k)$ for which $\tau_k(p^*) + r_i(p^*) = \tau_{k+1}(p^*)$, and all other indices satisfy the non-strict inequality condition in the previous paragraph. The number of impulses per period for the finite-dimensional system with parameter $p^*$ satisfies $n(p^*) < c + jc$, but if the ordering condition is satisfied for $p < p^*$, then the number of impulses per period at such parameters is $n(p) = j + jc$.

In Section 6, we will consider an example that exhibits different bifurcation diagrams depending on whether or not the ordering property is satisfied.

## 5. Transcritical bifurcation in a SIR model with unevently spaced impulsive treatment times

Consider the following simplistic SIR model of infectious disease transmission with impusive treatment leading to temporary immunity:

$$\dot{S} = wR - \beta(t, S, I), \quad t \neq \tau_k, \quad \Delta S = 0, \quad t = \tau_k \tag{SIR1}$$
$$\dot{I} = \beta(t, S, I) - rI \quad t \neq \tau_k, \quad \Delta I = -h(I), \quad t = \tau_k \tag{SIR2}$$
$$\dot{R} = -wR, \quad t \neq \tau_k \quad \Delta R = h(I), \quad t = \tau_k. \tag{SIR3}$$

In the above equations, $S, I$ and $R$ represent susceptible, infected and temporarily immune individuals, $\beta$ is the time-periodic infection rate with period $T$, $r$ is the rate at which individuals recover naturally and gain temporary immunity, $w$ is the rate at which temporary immunity is lost, $0 \leq h(I) \leq I$ is the number of individuals treated given $I$ infectives, and $\tau_k$ is a periodic sequence of times at which treatment occurs, with $\tau_{k+c} = \tau_k + T$. Note that pulse vaccination is not considered here, but one could readily modify the model to accommodate for this dynamic as well. Infectious disease model with pulse treatment have been considered in [Liu & Stechlinskli, 2012], among others.

It is simple to verify that in the above model, the total population size is constant; that is, $\frac{d}{dt}(S + I + R) = 0$ and $\Delta(S + I + R) = 0$. Consequently, one can eliminate the variable $R$ by setting $R = p - S - I$

for a parameter $p$ representing the population size. One then obtains the simplified model

$$\begin{aligned} \dot{S} &= wp - w(S+I) - \beta(t,S,I), \quad t \neq \tau_k, \qquad \Delta S = 0, \qquad t = \tau_k \\ \dot{I} &= \beta(t,S,I) - rI \qquad\qquad\quad t \neq \tau_k, \qquad \Delta I = -h(I), \quad t = \tau_k. \end{aligned}$$

We will now introduce some reasonable assumptions on the function $\beta$.

B.1 $\beta$ is $C^1$ in $S$ and $I$, and continuous in $t$;
B.2 $\beta(t,S,0) = 0$;
B.3 $\partial_I \beta(t,S,0) > 0$ for $S \neq 0$.

These conditions guarantee sufficient regularity to apply linearization and ensures that there is no net influx of new infective individuals when the population is infection-free, while an influx of infectives at nontrivial disease-free state will result in a higher infection rate. It follows that $\partial_S \beta(t,S,0) = 0$, and that $(S^*, I^*) = (p, 0)$ is an equilibrium point of the above impulsive system. The linearization at this equilibrium point produces the linear system

$$\dot{y} = \begin{bmatrix} -w & -w - \partial_I \beta(t,p,0) \\ 0 & \partial_I \beta(t,p,0) - r \end{bmatrix} y, \quad t \neq \tau_k \qquad \Delta y = \begin{bmatrix} 0 & 0 \\ 0 & -h'(0) \end{bmatrix} y, \quad t = \tau_k.$$

Due to the upper triangular structure of the above linear system, its Cauchy matrix $C(t,s)$ is also upper triangular, and its diagonal entries are given by

$$C_{ii}(t,s) = \begin{cases} e^{-w(t-s)}, & i = 1 \\ \exp\left(\int_s^t [\partial_I \beta(u,p,0) - r] du\right) \prod_{s \leq \tau_k < t} (1 - h'(0)), & i = 2. \end{cases}$$

The $(1,2)$ entry is more complicated and will not be needed at the moment. The monodromy matrix for the linearized system is upper triangular, and its eigenvalues are precisely $\mu_1 = C_{11}(\tau_0 + T, \tau_0)$ and $\mu_2 = C_{22}(\tau_0 + T, \tau_0)$. The first of these eigenvalues clearly satisfies $|\mu_1| < 1$, while for the second, it may be possible to have $|\mu_2| = 1$. Specifically, we have the following theorem, whose proof follows by linearized stability principles [Bainov & Simeonov, 1993].

**Theorem 3.** *Consider the SIR model* (SIR1)–(SIR3) *with seasonal infection rate of period $T$ and periodic treatment, with instants of treatment $\tau_k$ satisfying $\tau_{k+c} = \tau_k + T$; that is, there are $c$ instants of treatment per cycle. Let conditions B.1–B.2 be satisfied. For a given population size $p$, define*

$$\mu_2^p = \exp\left(\int_0^T \partial_I [\beta(t,p,0) - r] dt\right) \cdot (1 - h'(0))^c. \tag{28}$$

*The disease-free state is locally asymptotically stable if $\mu_2^p < 1$ and unstable if $\mu_2^p > 1$.*

When $\mu_2^p = 1$ for the Floquet multiplier appearing in equation (28), a fold-type bifurcation can occur. Since the function $h$ represents the strength of the treatment effort and $\mu_2^p$ depends on $h'(0)$, it seems reasonable that we take $h'(0)$ as a bifurcation parameter.The assumption $0 \leq h(I) \leq I$ together smoothness considerations and Taylor's theorem suggest we pose that

$$h(I,\lambda) = \lambda I + \frac{1}{2} h''(0,\lambda) I^2 + \frac{1}{6} h'''(0,\lambda) I^3 + O(I^4),$$

near $I = 0$ for $\lambda \in (0,1)$, where prime denotes differentiation in the variable $I$. With this representation, $h'(0,\lambda) = \lambda$, so we can identify $h'(0)$ with the bifurcation parameter, as desired. The critical parameter where $\mu_2^p$ is equal to one is therefore

$$\lambda^* = 1 - \exp\left(-\frac{1}{c} \int_0^T [\partial_I \beta(t,p,0) - r] dt\right). \tag{29}$$

We will henceforth assume $\lambda^* \in (0,1)$.

### 5.1. *Analysis of the case $\mu_2^P = 1$ by Lyapunov-Schmidt reduction*

Define the time-varying matrix function

$$A(t) = \begin{bmatrix} -w & -w - \partial_I \beta(t,p,0) \\ 0 & \partial_I \beta(t,p,0) - r \end{bmatrix}.$$

Also, let $E_{ij}$ denote the standard basis vectors for the space of $2 \times 2$ matrices, defined by $[E_{ij}]_{k\ell} = \delta_{ik}\delta_{j\ell}$. Denoting $X = (S, I)$, the first step in the Lyapunov-Schmidt reduction is to compute $D^X S((p,0),\lambda^*)$. We have $D^X S((p,0),\lambda^*) = [v^x(T)\ v^y(T)]$ where the functions $v^{x_i}$ satisfy the appropriate impulsive differential equations of Table 1. Specifically, written as a matrix, the function $C(t) = [v^x(t)\ v^y(t)]$ satisfies the linear impulsive differential equation

$$\begin{aligned} \dot{C} &= A(t)C, & t \neq \tau_k \\ \Delta C &= -\lambda^* E_{22} C, & t = \tau_k \\ C(0) &= I_{2\times 2}. \end{aligned}$$

The solution of the above initial-value problem satisfies, for $t > 0$ and $t \neq \tau_k$,

$$\begin{aligned} C(t) &= \begin{bmatrix} e^{-wt} - \int_0^t e^{-w(t-u)} \left[w + \partial_I \beta(u,p,0)\right] \exp\left(\int_0^u [\partial_I \beta(v,p,0) - r]dv\right) \cdot (1-\lambda^*)^{\#\{\tau_k \in [0,u)\}} du \\ 0 \qquad\qquad\qquad\qquad \exp\left(\int_0^t [\partial_I \beta(u,p,0) - r]du\right) \cdot (1-\lambda^*)^{\#\{\tau_k \in [0,t)\}} \end{bmatrix} \\ &= \begin{bmatrix} e^{-wt} - \int_0^t \frac{d}{du}\left[\exp\left(-w(t-u) + \int_0^u [\partial_I \beta(v,p,0) - r]dv\right)\right] \cdot (1-\lambda^*)^{\#\{\tau_k \in [0,u)\}} du \\ 0 \qquad\qquad\qquad\qquad \exp\left(\int_0^t [\partial_I \beta(u,p,0) - r]du\right) \cdot (1-\lambda^*)^{\#\{\tau_k \in [0,t)\}} \end{bmatrix}. \end{aligned}$$

Therefore, evaluating at $t = T$, we obtain

$$\begin{aligned} D^X S((p,0),\lambda^*) &= \begin{bmatrix} e^{-wT} & \kappa \\ 0 & 1 \end{bmatrix}, \\ \kappa &= -\int_0^T e^{-ru} \frac{d}{du}\left(\exp\left(-w(T-u) + \int_0^u \partial_I \beta(s,p,0) ds\right)\right) \cdot (1-\lambda^*)^{\sum_{k=0}^{c-1} H(u-\tau_k)} du, \end{aligned}$$

and $H(u)$ is the Heaviside function.

Now, define the operator $N : \mathbb{R}^2 \times \mathbb{R} \to \mathbb{R}^2$ by $N(X,\lambda) = S(x^* + X, \lambda^* + \lambda) - (x^* + X)$, $x^* = (p,0)$. It follows that $N(0,0) = S(x^*,\lambda^*) - x^* = 0$ and

$$D^X N(0,0) := \mathcal{N} = \begin{bmatrix} e^{-wT} - 1 & \kappa \\ 0 & 0 \end{bmatrix}, \quad r(\mathcal{N}) = \operatorname{span}\begin{bmatrix} 1 \\ 0 \end{bmatrix} \quad \ker(\mathcal{N}) = \operatorname{span}\begin{bmatrix} \kappa \\ 1 - e^{-wT} \end{bmatrix}.$$

Consequently, a (orthogonal) projection onto the range of $\mathcal{N}$ is given by $P = E_{11}$. This projection will be useful later. This effective change of variables identifies $\lambda = \lambda^*$ with respect to the map $S$ with $\lambda = 0$ with respect to the $N$ map; this distinction will be important later on.

Next, we compute $D^\lambda S(x^*,\lambda^*)$. The function $v^\lambda(t)$ satisfies the differential equation

$$\begin{aligned} \dot{v}^\lambda &= A(t)v^\lambda, & t \neq \tau_k \\ \Delta v^\lambda &= -\lambda^* E_{22} v^\lambda, & t = \tau_k \\ v^\lambda(0) &= 0. \end{aligned}$$

Therefore, $v^\lambda(T) = 0$, which implies that $D^\lambda S(x^*,\lambda^*) = v^\lambda(T^-) = 0$ and, consequently, $D^\lambda N(0,0) = 0$. In fact, we can say more; if $\lambda \in (0,1)$ is given, then one has that $\lambda \mapsto S((p,0),\lambda)$ is constant because $\dot{I} = 0$ and $\Delta I = 0$ along the orbit through $(p,0)$. Therefore, $D^{\lambda^n} N(0,0) = 0$.

For the computation of $D^{X\lambda} S(x^*,\lambda^*)$, we must solve the impulsive differential equation

$$\begin{aligned} \dot{v}^{X\lambda} &= A(t)v^{X\lambda}, & t \neq \tau_k \\ \Delta v^{X\lambda} &= -\lambda^* E_{22} v^{X\lambda} - C_{22}(\tau_k) E_{22}, & t = \tau_k \\ v^{X\lambda}(0) &= 0. \end{aligned}$$

Note that the above equation follows by applying Table 1 to each column of $D^{X\lambda}S(x^*,\lambda^*)$ and then collecting the columns in a single matrix impulsive differential equation. The solution is given for $t \in (0,T)\setminus\{\tau_k\}$ by

$$v^{X\lambda}(t) = -C(t)\sum_{0\le\tau_k<t} C^{-1}(\tau_k^+)C_{22}(\tau_k)E_{22}.$$

Therefore, we may calculate $D^{X\lambda}N(0,0)$ as

$$\begin{aligned}
D^{X\lambda}N(0,0) &= v^{X\lambda}(T^-)\\
&= -D^X S(x^*,\lambda^*)\sum_{k=0}^{c-1} C_{22}^{-1}(\tau_k^+)C_{11}^{-1}(\tau_k^+)\mathrm{Adj}(C(\tau_k^+))C_{22}(\tau_k)E_{22}\\
&= -\frac{1}{1-\lambda^*}D^X S(x^*,\lambda^*)\sum_{k=0}^{c-1} e^{w\tau_k}\mathrm{Adj}((C(\tau_k^+))E_{22}\\
&= -\frac{1}{1-\lambda^*}D^X S(x^*,\lambda^*)\sum_{k=0}^{c-1}((-e^{w\tau_k}C_{12}(\tau_k))E_{12}+E_{22})\\
&= -\frac{1}{1-\lambda^*}\left(\sum_{k=0}^{c-1}\kappa - e^{w(\tau_k-T)}C_{11}(\tau_k)\right)E_{12} + \frac{c}{1-\lambda^*}E_{22}\\
&= -\frac{c(\kappa-e^{-wT})}{1-\lambda^*}E_{12} - \frac{c}{1-\lambda^*}E_{22}
\end{aligned}$$

which implies that

$$D^{S\lambda}N(0,0) = 0, \qquad D^{I\lambda}N(0,0) = -\frac{c}{1-\lambda^*}\begin{bmatrix}\kappa - e^{-wT}\\ 1\end{bmatrix}.$$

The final partial derivatives are those of the form $D^{x_ix_j}N(0,0)$ for $x_i,x_j\in\{S,I\}$. Applying Table 1, we have

$$\begin{aligned}
\dot v^{x_ix_j} &= A(t)v^{x_ix_j} + (v_1^{x_i}v_2^{x_j} + v_2^{x_i}v_1^{x-j})\begin{bmatrix}-\partial_{SI}\beta\\ \partial_{SI}\beta\end{bmatrix} + v_2^{x_i}v_2^{x_j}\begin{bmatrix}-\partial_{II}\beta\\ \partial_{II}\beta\end{bmatrix}, \quad t\neq\tau_k\\
\Delta v^{x_ix_j} &= -\lambda^* E_{22}v^{x_ix_j} + v_2^{x_i}v_2^{x_j}\begin{bmatrix}0\\ -h''(0,\lambda^*)\end{bmatrix}, \qquad t=\tau_k\\
v^{x_ix_j}(0) &= 0,
\end{aligned}$$

where all partial derivatives of $\beta$ are evaluated at $\beta(t,p,0)$ and we have used the fact that $\partial_{SS}\beta(t,p,0)=0$. Beginning with $v^{SS}$, since $v_2^S(t)=0$ for all $t$, we see that $v^{SS}$ satisfies

$$\begin{aligned}
\dot v^{SS} &= A(t)v^{SS}, \qquad t\neq\tau_k\\
\Delta v^{SS} &= -\lambda^* E_{22}v^{SS}, \quad t=\tau_k\\
v^{SS}(0) &= 0,
\end{aligned}$$

and consequently $D^{SS}N(0,0)=v^{SS}(T)=0$. Next, we compute $D^{SI}N(0,0)$. Solving the impulsive differential equation

$$\begin{aligned}
\dot v^{SI} &= A(t)v^{SI} + \partial_{SI}\beta(t,p,0)C_{11}(t)C_{22}(t)(-e_1+e_2), \quad t\neq\tau_k\\
\Delta v^{SI} &= -\lambda^* E_{22}v^{SI}, \qquad t=\tau_k\\
v^{SI}(0) &= 0,
\end{aligned}$$

we obtain the representation

$$D^{SI}N(0,0) = D^X S(x^*,\lambda^*)\int_0^T \partial_{SI}\beta(s,p,0)C_{11}(s)C_{22}(s)C^{-1}(s)(-e_1+e_2)ds := \begin{bmatrix}c_1^{SI}\\ c_2^{SI}\end{bmatrix} \tag{30}$$

Finally, to compute $D^{II}N(0,0)$, we solve

$$\begin{aligned}
\dot{v}^{II} &= A(t)v^{II} + 2\partial_{SI}\beta(t,p,0)C_{12}(t)C_{22}(t)(-e_1+e_2) + \partial_{II}\beta(t,p,0)C_{22}^2(t)(-e_1+e_2), && t \neq \tau_k \\
\Delta v^{II} &= -\lambda^* E_{22}v^{II} - h''(0,\lambda^*)C_{22}^2(\tau_k)e_2 && t = \tau_k \\
v^{II}(0) &= 0,
\end{aligned}$$

thereby obtaining

$$\begin{aligned}
D^{II}N(0,0) =& D^X S(x^*,\lambda^*)\left[\int_0^T \left(2\partial_{SI}\beta(s,p,0)C_{12}(s)C_{22}(s) + \partial_{II}\beta(s,p,0)C_{22}^2(s)\right)C^{-1}(s)(-e_1+e_2)ds\right. \\
&\left. - h''(0,\lambda^*)\sum_{k=0}^{c-1} C_{22}^2(\tau_k)C^{-1}(\tau_k^+)e_2\right] \\
:=& \begin{bmatrix} c_1^{II} \\ c_2^{II} \end{bmatrix}.
\end{aligned} \tag{31}$$

With all of the above calculations and notation in place, we see that the function $N(x,\lambda)$ can be written

$$N(S,I,\lambda) = \begin{bmatrix} e^{-wT}-1 & \kappa \\ 0 & 0 \end{bmatrix}\begin{bmatrix} S \\ I \end{bmatrix} + \frac{c}{1-\lambda^*}\begin{bmatrix} \kappa - e^{-wT} \\ 1 \end{bmatrix}\lambda I + \begin{bmatrix} c_1^{SI}SI + \frac{c_1^{II}}{2}I^2 \\ c_2^{SI}SI + \frac{c_2^{II}}{2}I^2 \end{bmatrix} + O^3(S,I,\lambda), \tag{32}$$

$$\kappa = -\int_0^T e^{-ru}\frac{d}{du}\left(\exp\left(-w(T-u) + \int_0^u \partial_I\beta(s,p,0)ds\right)\right)\cdot(1-\lambda^*)^{\sum_{k=0}^{c-1}H(u-\tau_k)}du, \tag{33}$$

where $O^q(Z)$ denotes terms of order $q$ or higher in the variable $Z$ and $H(u)$ is the Heaviside function. Notice that under assumption B.3, one has $\kappa < 0$. Applying the projection operator $P = E_{11}$ to both sides of the equation $N(S,I,\lambda) = 0$, we obtain

$$(e^{-wT}-1)S + \kappa I + \frac{c(\kappa - e^{-wT})}{1-\lambda^*}\lambda I + c_1^{SI}SI + \frac{c_1^{II}}{2}I^2 + O^3(S,I,\lambda) = 0, \tag{34}$$

where the second component of the vector is identically zero and has been neglected. By the implicit function theorem, there exists a unique smooth function $\overline{S}(I,\lambda)$ such that $(\overline{S}(I,\lambda),I,\lambda)$ solves equation (34) for $(\lambda,I) \approx (0,0)$, with the property that $\overline{S}(0,0) = 0$. Implicitly differentating both sides of (34) with respect to the variable $I$ and $\lambda$, we find that

$$\partial_I\overline{S}(0,0) = \frac{\kappa}{1-e^{-wT}}, \qquad \overline{S}_\lambda(0,0) = 0. \tag{35}$$

The bifurcation equation (11) is therefore

$$I\left(-\frac{c}{1-\lambda^*}\lambda + c_2^{SI}\overline{S}(I,\lambda) + \frac{c_2^{II}}{2}I + O^2(\lambda,I)\right) = 0, \tag{36}$$

where $S$ does not appear explicitly in the higher-order terms because of the reduction $S = \overline{S}(I,\lambda)$. Notice that we are able to bring the higher-order terms inside the parentheses because all higher-order terms of the form $r_n\lambda^n$ vanish because we have proven that $D^{\lambda^n}N(0,0) = 0$. The structure of the term in the parentheses determines the branches $I = I(\lambda)$ of nontrivial periodic solutions of the SIR model. By the implicit function theorem (applied to the parenthetical part), a nontrivial branch $I = I(\lambda)$ exists near $\lambda = 0$ and, consequently, a unique nontrivial periodic solution bifurcates at $\lambda = \lambda^*$ in a transcritical bifurcation, assuming the condition

$$\zeta := \frac{\kappa c_2^{SI}}{1-e^{-wT}} + \frac{c_2^{II}}{2} \neq 0 \tag{37}$$

holds. With slightly more analysis, we can prove the following.

**Theorem 4.** *Under generic conditions ($\zeta \neq 0$), the seasonal SIR model satisfying conditions B.1–B.2 with impulsive treatment and temporary immunity and smooth treatment function $h(I,\lambda) = -\lambda I + O(I^2)$ undergoes a transcritical bifurcation at the disease-free equilibrium when $\lambda = \lambda^*$, for the parameter $\lambda^*$ appearing in* (29)*. If $\lambda^* < 1$, the bifurcating periodic orbit is nonnegative for $\lambda \approx \lambda^*$ only when $(\lambda - \lambda^*)\zeta > 0$.*

*Proof.* We first prove that the condition $\zeta \neq 0$ is generic. Notice that $c_2^{SI}\partial_I \overline{S}(0,0)$ as appearing in the condition (37) is independent of $h''(0,\lambda^*) = \partial_{II}h(0,\lambda^*)$. The dependence of the $c_2^{II}$ on $h''(0,\lambda^*)$ will now be investigated. Examining equation (31), it is readily verified that

$$c_2^{II} = R - e_2^T D^X S(x^*,\lambda^*) h''(0,\lambda^*) \sum_{k=0}^{c-1} C_{22}^2(\tau_k) C^{-1}(\tau_k^+) e_2 := R - R_h$$

for some $R$ independent of $h''(0,\lambda^*)$. To compute the other term ($R_h$), we begin by simplifying the summation. Note first that that $C_{22}^2(\tau_k)C^{-1}(\tau_k) = \frac{1}{1-\lambda^*} C_{22}(\tau_k) e^{w\tau_k} \mathrm{Adj}(C(\tau_k))$. Then, we have

$$\begin{aligned}\sum_{k=0}^{c-1} C_{22}^2(\tau_k) C^{-1}(\tau_k^+) &= \frac{1}{1-\lambda^*} \sum_{k=0}^{c-1} C_{22}(\tau_k) e^{w\tau_k} \begin{bmatrix} e^{-wT} & \kappa \\ 0 & 1 \end{bmatrix} \begin{bmatrix} C_{22}(\tau_k) & -C_{12}(\tau_k) \\ 0 & e^{-w\tau_k} \end{bmatrix} \\ &= \frac{1}{1-\lambda^*} \sum_{k=0}^{c-1} C_{22}(\tau_k) \begin{bmatrix} \cdot & \cdot \\ 0 & 1 \end{bmatrix},\end{aligned}$$

where the $(1,1)$ and $(1,2)$ entries will not be needed because we will be conjugating by $e_2$, and only the $(2,2)$ entry will remain. Then, $R_h$ is given by

$$R_h = \frac{h''(0,\lambda^*)}{1-\lambda^*} \sum_{k=0}^{c-1} C_{22}(\tau_k) = h''(0,\lambda^*) \sum_{k=0}^{c-1} (1-\lambda^*)^k \exp\left( \int_0^{\tau_k} [\partial_I \beta(t,p,0) - r] dt \right).$$

Since the terms inside the summation are strictly positive, it follows that $R_h$, and hence $c_2^{II}$, depends linearly and nontrivially on $h''(0,\lambda^*)$. Therefore, condition $\zeta \neq 0$ of (36) is generic.

To prove the assertion concerning the sign of the periodic orbit, we note that the linear approximation $I(\lambda) = \frac{c}{\zeta(1-\lambda^*)}\lambda + O(\lambda^2)$ is with respect to zeroes of the map $N$, so that

$$I(\lambda) = \frac{c}{\zeta(1-\lambda^*)}(\lambda - \lambda^*) + O((\lambda-\lambda^*)^2) \tag{38}$$

as a fixed point of the stroboscopic map, with the original coordinate system on the parameter. The sign of $I(\lambda)$ near $\lambda^*$ is therefore equivalent to that of $(\lambda - \lambda^*)\zeta$, since it is assumed that $\lambda^* \in (0,1)$. Therefore, $I(\lambda) > 0$ near $\lambda^*$ only if $(\lambda - \lambda^*)\zeta > 0$. The sign of $S$ is positive regardless because

$$S(\lambda) = p + \frac{\kappa}{1-e^{-wT}} I(\lambda) + O((\lambda-\lambda^*)^2),$$

which implies $S > 0$ near $\lambda = \lambda^*$. ■

The example of this section is noteworthy because, to our knowledge, there are no examples in the literature of an impulsive model that is explicitly proven to undergo a bifurcation in a case where the impulse times are not evenly spaced. To determine the stability of the bifurcating periodic orbit, we must either approximate the periodic orbit and compute its linearization or use center manifold reduction. To approximate it, one may use the linear approximation described in the proof of Theorem 4. Alternatively, a quicker way to infer stability in this case is to notice that since the bifurcation is transcritical, the stability of the fixed point at the origin must be the opposite of that of the bifurcating fixed point. Thus, the bifurcating (coexistence) periodic orbit is stable when $\lambda < \lambda^*$, and unstable when $\lambda > \lambda^*$.

### 5.2. *Analysis of the case $\mu_2^P = 1$ by Center Manifold Reduction*

Since we consider bifurcation from an equilibrium point, we are in the case of a periodic orbit of period $T(\lambda^*)$, so in the notation of Section 3.2, we have the case of an order $k = 1$ composition. Therefore, $U^1(x,\lambda) = S(x + x^*, \lambda + \lambda^*) - x^* = N(x,\lambda) + x$, so the second-order terms and higher of $U^1$, the function for which we need to compute a Taylor expansion, will coincide with those of $N(x,\lambda)$ from Section 5.1. Also, since we already know that $D^\lambda N(0,0) = 0$ from the aforementioned section, the third column of $D\mathbf{U}(0,0)$ will be precisely $[0\ 0\ 1]^T$, where the 1 in the third component comes from the derivative of $\lambda \mapsto \lambda$ with respect to $\lambda$. Therefore, the map $(S, I, \lambda) \mapsto \mathbf{U}(S, I, \lambda)$ has the expansion

$$\begin{bmatrix} S \\ I \\ \lambda \end{bmatrix} \mapsto \begin{bmatrix} e^{-wT} & \kappa & 0 \\ 0 & 1 & 0 \\ 0 & 0 & 1 \end{bmatrix} \begin{bmatrix} S \\ I \\ \lambda \end{bmatrix} - \frac{c}{1-\lambda^*} \begin{bmatrix} \kappa - e^{-wT} \\ 1 \\ 0 \end{bmatrix} \lambda I + \begin{bmatrix} c_1^{SI} SI + \frac{c_1^{II}}{2} I^2 \\ c_2^{SI} SI + \frac{c_2^{II}}{2} I^2 \\ 0 \end{bmatrix} + O((S,I,\lambda)^3),$$

where we have suppressed indices on $S, I, \lambda$ and written the discrete-time ssytem with iterated map convention. The Jordan normal form $D\mathbf{U}(0,0) = PJP^{-1}$ is

$$D\mathbf{U}(0,0) = \begin{bmatrix} 1 & \kappa & 0 \\ 0 & 1 - e^{-wT} & 0 \\ 0 & 0 & 1 \end{bmatrix} \operatorname{diag}(e^{-wT}, 1, 1) \begin{bmatrix} 1 & \kappa(1-e^{-wT})^{-1} & 0 \\ 0 & -(1-e^{-wT})^{-1} & 0 \\ 0 & 0 & 1 \end{bmatrix},$$

and upon applying the transformation $[S\ I\ \lambda]^T = P[y\ \lambda]^T$, one obtains

$$\begin{aligned} y_1 &\mapsto e^{-wT} y_1 - c\frac{(\kappa - e^{-wT})(1-e^{-wT}) - \kappa}{1-\lambda^*}\lambda y_2 + \left(\frac{c_1^{SI}}{1-e^{-wT}} - \kappa c_2^{SI}\right) y_1 y_2 \\ &\quad + \left(\frac{c_1^{SI}\kappa}{1-e^{-wT}} + \frac{c_1^{II}(1-e^{-wT})^2}{2} - c_2^{SI}\kappa^2 - \frac{\kappa c_2^{II}(1-e^{-wT})}{2}\right) y_2^2 \\ y_2 &\mapsto y_2 - \frac{c}{1-\lambda^*}\lambda y_2 + c_2^{SI} y_1 y_2 + \left(c_2^{SI}\kappa + \frac{c_2^{II}}{2(1-e^{-wT})}\right) y_2^2 \\ \lambda &\mapsto \lambda. \end{aligned} \tag{39}$$

Let $y_1 = h(y_2, \lambda) = h_{20} y_2^2 + h_{11} y_2 \lambda + h_{02}\lambda^2 + O((y_2,\lambda)^3)$ be a quadratic approximation to the center manifold. Substituting $y_1 = h(y_2,\lambda)$ and the transformed equation (39) into the invariance condition (19) and comparing quadratic terms on the left- and right-hand sides, we find

$$\begin{aligned} y_2^2: &\quad e^{-wT} h_{20} + \left(\frac{c_1^{SI}\kappa}{1-e^{-wT}} + \frac{c_1^{II}(1-e^{-wT})^2}{2} - c_2^{SI}\kappa^2 - \frac{\kappa c_2^{II}(1-e^{-wT})}{2}\right) = h_{20}, \\ \lambda y_2: &\quad e^{-wT} h_{11} - c\frac{(\kappa - e^{-wT})(1-e^{-wT}) - \kappa}{1-\lambda^*} = h_{11}, \\ \lambda^2 &\quad e^{-wT} h_{02} = h_{02}. \end{aligned}$$

Since $e^{-wT} \neq 1$, these equations are uniquely solvable for $h_{20}$, $h_{11}$ and $h_{02}$. Leaving the coefficients as implicit, the dynamics reduced to the center manifold are given by

$$y_2 \mapsto y_2 - \frac{c}{1-\lambda^*}\lambda y_2 + c_2^{SI}(h_{20} y_2^2 + h_{11} y_2 \lambda + h_{02}\lambda^2) y_2 + \left(c_2^{SI}\kappa + \frac{c_2^{II}}{2(1-e^{-wT})}\right) y_2^2 + O((y_2,\lambda)^3).$$

By truncating the above map to order two and simplifying, we obtain

$$y_2 \mapsto y_2 - \frac{c}{1-\lambda^*}\lambda y_2 + \frac{\zeta}{1-e^{-wT}} y_2^2 + O((y_2,\lambda)^3), \tag{40}$$

and all of the coefficients $h_{ij}$ vanish. A transcritical bifurcation occurs if the quadratic term is nonzero [Wiggins, 2003]. See the associated bifurcation diagram: Figure 5.2. This is in agreement with the condition $\zeta \neq 0$ obtained by Lyapunov-Schmidt reduction: equation (37). However, we gain more information here because the center manifold reduction maintains the dynamics and stability results, while the Lyapunov-Schmidt

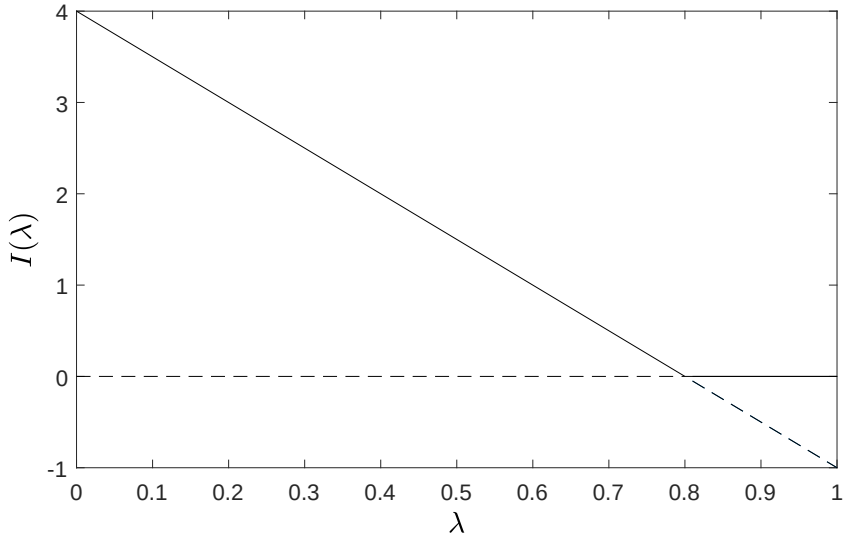


Fig. 1. The (local) bifurcation diagram for the SIR model with irregularly-spaced impulsive treatment times at the disease-free equilibrium, with illustrative parameters resulting in $\lambda^* = 0.8$ and $\zeta < 0$. The diagonal line corresponds to the nontrivial branch of periodic solutions; specifically, it is the linear approximation to $I(\lambda)$ as given in equation (38) at $\lambda = \lambda^*$. The horizontal line is the disease-free equilibrium. The vertical axis represents the infected component $I$. Due to the change of variables $I = (1-e^{-wT})y_2$, the above diagram is identical (up to translation in $\lambda$ and rescaling in $I$) to the bifurcation diagram of the quadratic order approximation of the center manifold dynamics (40). Asymptotically stable states are indicated by solid lines, with unstable states as dashed lines.

reduction does not generally grant stability results directly. For equation (40), the critical parameter is $\lambda = 0$ (in the original system, this corresponds to $\lambda = \lambda^*$; recall that we originally performed a linear change of variables to translate $\lambda^*$ to the origin). We see that the fixed point $y_2 = 0$ is stable when $\lambda > 0$ and unstable when $\lambda < 0$, while when $\lambda = 0$, the fixed point is stable from the $-\text{sgn}(\zeta)$ direction. As for the bifurcating fixed point, $y_2^*$, it follows by the implicit function theorem that

$$y_2^*(\lambda) = \frac{c(1-e^{-wT})}{\zeta(1-\lambda^*)}\lambda + O(\lambda^2),$$

and one can then calculate directly (by linearizing (40) at $y_2^*(\lambda)$) that the linearization at this fixed point is

$$z \mapsto \lambda\left(\frac{c}{1-\lambda^*} + O(\lambda)\right) z.$$

Therefore, the $y_2^*(\lambda)$ is stable when $\lambda < 0$ and unstable when $\lambda > 0$. Also, from the expression for $y_2^*(\lambda)$, we see once again that $y_2^*(\lambda) > 0$ for $\lambda$ small only if $\lambda\zeta > 0$. To conclude, we have the following theorem, which refines Theorem 4.

**Theorem 5.** *Under generic conditions ($\zeta \neq 0$), the seasonal SIR model with impulsive treatment and temporary immunity with smooth treatment function $h(I, \lambda) = -\lambda I + O(I^2)$ undergoes a transcritical bifurcation at the disease-free equilibrium when $\lambda = \lambda^*$. Specifically, the following hold locally for $|\lambda - \lambda^*|$ small.*

*(1) If $\lambda < \lambda^*$, the disease-free equilibrium is unstable, while it is asymptotically stable if $\lambda > \lambda^*$.*
*(2) If $\zeta < 0$, there is a (nonnegative) coexistence periodic orbit when $\lambda < \lambda^*$ that is asymptotically stable. When $\lambda > \lambda^*$, there is a neighbourhood about the disease-free equilibrium in which there are no nontrivial nonnegative periodic orbits.*
*(3) If $\zeta > 0$, there is a (nonnegative) coexistence periodic orbit when $\lambda > \lambda^*$ that is unstable. When $\lambda < \lambda^*$, there is a a neighbourhood about the disease-free equilibrium in which there are no nontrivial nonnegative periodic orbits.*

In the degenerate case where $\zeta = 0$, a pitchfork bifurcation may occur, as can be verified by normal form theory [Wiggins, 2003]. We do not indend on checking the nondegeneracy condition for the pitchfork bifurcation because this would necessitate computing a higher-order approximation of the stroboscopic map, and we have already shown that the condition $\zeta \neq 0$ is generic; see Theorem 4

## 6. Logistic equation with delayed impulsive harvesting

The example of this section is inspired by the delayed logistic map, which can be shown to undergo a Neimark-Sacker bifurcation [Kuznetsov, 2004]. We consider here a logistic differential equation that does not exhibit delays, but for which a harvesting effort acts on the delayed population census. As such, it can be considered a generalization of the model considered in [Zhang, Shuai and Wang, 2003], for example. The model reads as follows.

$$\dot{x} = rx(1 - x/N), \qquad t \neq kT \tag{41}$$
$$\Delta x = -\epsilon x(t - \omega), \qquad t = kT. \tag{42}$$

$r > 0$ is the intrinsic growth rate, $N > 0$ the carrying capacity, $T > 0$ the harvesting period, $\epsilon \in (0, 1)$ the harvesting effort, and $\omega \in (0, T]$ the census delay, and $k \in \mathbb{Z}$. Applying the method of Section 4, the above is equivalent to the two-dimensional system without impulses:

$$\dot{x} = rx(1 - x/N), \qquad t \notin \{kT, kT - \omega\} \tag{43}$$
$$\dot{y} = 0, \qquad t \notin \{kT, kT - \omega\} \tag{44}$$
$$\Delta x = -\epsilon y, \qquad t = kT \tag{45}$$
$$\Delta y = x - y, \qquad t = kT - \omega. \tag{46}$$

Note that for $\omega < T$, the sequence of impulses can be identified with $\tau_j = \lfloor j/2 \rfloor T - [j + 1]_2\omega$. With this identification,

$$\tau_{j+2} = \left\lfloor \frac{j}{2} + 1 \right\rfloor T - [j + 3]_2\omega = (1 + \lfloor j/2 \rfloor)T - [j + 1]_2\omega = \tau_j + T,$$

and the impulsive system (43)–(46) is periodic with period $T$ and two impulses per period.

The case where $\omega = T$ is slightly more subtle. Impulses occur at the times $\{kT, (k - 1)T : k \in \mathbb{Z}\} = \{kT : k \in \mathbb{Z}\}$. Thus, the sequence of impulses can be identified with $\tau_j = jT$ so that the period is $T$ and there is only one impulse per period. The jump of population state $x$ and the reset action for the delayed state $y$ overlap in this case, and we will see in Section 6.2 that although the biologically meaningful orbit structure is the same as in the case where $\omega \neq T$, mathematically, the complete orbit structure is more rich.

### 6.1. *The case $\omega \neq T$*

The extinction state, $(x, y) = (0, 0)$, is an equilibrium point of (43)–(46). The linearization at this equilibrium produces the linear system

$$\begin{aligned} \dot{z} &= rz, && t \notin \{kT, kT - \omega\} \\ \dot{w} &= 0, && t \notin \{kT, kT - \omega\} \\ \Delta z &= -\epsilon w, && t = kT \\ \Delta w &= z - w, && t = kT - \omega. \end{aligned} \tag{47}$$

Note that the first two impulse times occur at time $t = 0$ and time $t = T - \omega$. The monodromy matrix is

$$M_\omega(\epsilon) = \begin{bmatrix} e^{rT} & -\epsilon e^{rT} \\ e^{r(T-\omega)} & -\epsilon e^{r(T-\omega)} \end{bmatrix}.$$

$M_\omega(\epsilon)$ is not invertible, so the eigenvalues are precisely $\mu_1 = 0$ and $\mu_2 = e^{rT}(1 - \epsilon e^{-r\omega})$.

Treating $\epsilon$ as a parameter, we have $\mu_2 = 1$ when $\epsilon = \epsilon^*$:

$$\epsilon^* = e^{r\omega}(1 - e^{-rT}). \tag{48}$$

We expect a transcritical or pitchfork bifurcation to occur due to the stationary fixed point at the origin. We will use the method of Lyapunov-Schmidt reduction, since it is computationally faster and we do not require the more sophisticated center manifold reduction here because the critical Floquet multiplier is not complex.

Using Table 1, we have that the differential equations for the function $v^X$ for $X = (x, y)$ is simply the variational equation (47) with initial condition $v^X(0) = I$. For $t \in (0, T]$, we have

$$v^X(t) = \begin{bmatrix} e^{rt} & -\epsilon^* e^{rt} \\ e^{r(T-\omega)}\mathbb{1}_{(T-\omega.T]} & 1 - (1 + \epsilon^* e^{r(T-\omega)})\mathbb{1}_{(T-\omega,T]} \end{bmatrix} = [\, v^x(t)\ v^y(t)\,].$$

Also, one easily finds $v^{\epsilon^k}(t) = 0$ for all $k \geq 1$ because the equilibrium at the origin is independent of the parameter $\epsilon$.

The second-order terms are somewhat more complicated. Table 1 yields the system

$$\begin{aligned}
\dot{v}^{\alpha\beta} &= rE_{11}v^{\alpha\beta} - e_1\frac{2r}{N}v_x^\alpha v_x^\beta, && t \notin \{kT, kT-\omega\},\ \alpha\beta \in \{xx, xy, yy, x\epsilon, y\epsilon\} \\
\Delta v^{\alpha\beta} &= -\epsilon^* E_{12}v^{\alpha\beta}, && t = kT,\ \alpha\beta \in \{xx, xy, yy, x\epsilon\} \\
\Delta v^{y\epsilon} &= -\epsilon^* E_{12}v^{y\epsilon} - E_{12}v^y, && t = kT \\
\Delta v^{\alpha\beta} &= (E_{21} - E_{22})v^{\alpha\beta}, && t = kT-\omega,\ \alpha\beta \in \{xx, xy, yy, x\epsilon, y\epsilon, \epsilon\epsilon\},
\end{aligned}$$

all with identical initial conditions $v^{\alpha\beta}(0) = 0$. The complete solution is given for $t \in (0, T]$ as

$$\begin{aligned}
v^{xx}(t) &= \begin{bmatrix} -\frac{2}{N} \cdot e^{rt}(e^{rt} - 1) \\ -\mathbb{1}_{(T-\omega,T]}\frac{2}{N} \cdot e^{r(T-\omega)}(e^{r(T-\omega)} - 1) \end{bmatrix}, \quad v^{y\epsilon}(t) = \begin{bmatrix} -e^{rt} \\ -\mathbb{1}_{(T-\omega,T]}e^{r(T-\omega)} \end{bmatrix}, \\
v^{xy}(t) &= -\epsilon^* v^{xx}(t), \qquad v^{x\epsilon}(t) = 0, \\
v^{yy}(t) &= (\epsilon^*)^2 v^{xx}(t)
\end{aligned}$$

Since the impulse times do not depend on the parameter, one can formally differentiate the appropriate rows of Table 1 following Section 2.3.2 to obtain

$$\begin{aligned}
\dot{v}^{y^j\epsilon^k} &= rE_{11}v^{y^j\epsilon^k}, && t \notin \{kT, kT-\omega\} \\
\Delta v^{y^j\epsilon^k} &= -\epsilon^* E_{12}v^{y^j\epsilon^k}, && t = kT \\
\Delta v^{y^j\epsilon^k} &= (E_{21} - E_{22})v^{y^j\epsilon^k}, && t = kT-\omega,
\end{aligned}$$

for any $j + k \geq 3$. Since the initial conditions are all zero, we conclude that $v^{y^j\epsilon^k}(t) = 0$ for $j + k \geq 3$. Therefore, the map $N = S - I$, where $S = S(x, y, \epsilon)$ is the stroboscopic map, has near $(x, y, \epsilon) = (x, y, \epsilon^*)$ the approximation

$$N(x, y, \epsilon) = (M_\omega(\epsilon^*) - I)\begin{bmatrix} x \\ y \end{bmatrix} + \begin{bmatrix} \frac{1}{2}v_x^{xx}(T)x^2 - \epsilon^* v_x^{xx}(T)xy + \frac{(\epsilon^*)^2}{2}v_x^{xx}y^2 - e^{rT}y\bar{\epsilon} \\ \frac{1}{2}v_y^{xx}(T)x^2 - \epsilon^* v_y^{xx}(T)xy + \frac{(\epsilon^*)^2}{2}v_y^{xx}(T)y^2 - e^{r(T-\omega)}y\bar{\epsilon} \end{bmatrix} + O(x^3) + yO^2(y, \bar{\epsilon}), \tag{49}$$

with $\bar{\epsilon} = \epsilon - \epsilon^*$. We could compute the projection onto the range of $M_\omega(\epsilon^*) - I$ and continue applying the Lyapunov-Schmidt method verbatim, but this is not necessary here because by inspection, we note that the second row is implicitly sovable for $x = x(y, \epsilon)$. Specifically, the second row of $N(x, y, \epsilon) = 0$ is given by

$$e^{r(T-\omega)}x - e^{rT}y + \frac{1}{2}v_y^{xx}(T)x^2 - \epsilon^* v_y^{xx}(T)xy + \frac{(\epsilon^*)^2}{2}v_y^{xx}(T)y^2 - e^{r(T-\omega)}y\bar{\epsilon} + O(x^3) + yO^2(y, \bar{\epsilon}) = 0.$$

As $\partial_x N_2(0,0,\epsilon^*) \neq 0$, the implicit function theorem applies. In particular, by implicitly differentiating the above equation, we can obtain the representation

$$x = x(y,\epsilon) = y\left(e^{r\omega} + \overline{\epsilon} + \epsilon^* e^{-r(T-\omega)} v_y^{xx}(T)\left[e^{r\omega} + \frac{\epsilon^*}{2}\right] y\right) := yF(y,\overline{\epsilon}),$$

which is correct to order $yO^2(y,\overline{\epsilon})$. Substituting the above into the first row of (49) results in the equation

$$(e^{rT}-1)F(y,\overline{\epsilon})y - e^{r\omega}(e^{rT}-1)y + \frac{1}{2}v_x^{xx}(T)F^2(y,\overline{\epsilon})y^2 - \epsilon^* v_x^{xy}F(y,\overline{\epsilon})y^2 + \frac{\epsilon^*}{2}v_x^{xx}y - e^{rT}\overline{\epsilon}y + yO^2(y,\overline{\epsilon}) = 0$$

If we seek nontrivial bifurcating solutions, we can factor out a $y$ term. Then, one obtains

$$\begin{aligned}\frac{N(x(y,\epsilon),y,\epsilon)}{y} &= (e^{rT}-1)F(y,\overline{\epsilon}) - e^{r\omega}(e^{rT}-1) + \frac{1}{2}v_x^{xx}(T)F^2(y,\overline{\epsilon})y - \epsilon^* v_x^{xy}F(y,\overline{\epsilon})y + \frac{\epsilon^*}{2}v_x^{xx} - e^{rT}\overline{\epsilon} \\ &= -\overline{\epsilon} + y\left((e^{rT}-1)\epsilon^* e^{-r(T-\omega)}\left[e^{r\omega}+\frac{\epsilon^*}{2}\right]v_y^{xx}(T) + \left(\frac{e^{2r\omega}}{2} - \epsilon^* e^{r\omega} + \frac{(\epsilon^*)^2}{2}\right)v_x^{xx}(T)\right) \\ &:= -\overline{\epsilon} + yY(\epsilon^*)\end{aligned}$$

plus terms of order $O^2(y,\overline{\epsilon})$. The implicit function theorem implies that a unique, nontrivial branch of periodic solutions bifurcates at $\epsilon = \epsilon^*$, and the nontrivial fixed point of the stroboscopic map is given to linear order by the equation

$$(x,y) = \left((e^{r\omega} + \epsilon - \epsilon^*)y, \frac{\epsilon - \epsilon^*}{Y(\epsilon^*)}\right). \tag{50}$$

Notice that $Y(\epsilon^*)$ is negative, so the nontrivial periodic orbit is is positive if $\epsilon < \epsilon^*$, while when $\epsilon > \epsilon^*$, it is negative. To analyze stability, one may note that the nonzero eigenvalue of $M_\omega(\epsilon)$ has modulus less than one when $\epsilon > \epsilon^*$, while it has modulus greater than one when $\epsilon < \epsilon^*$. Consequently, the bifurcating periodic orbit is stable when $\epsilon < \epsilon^*$ and is unstable when $\epsilon > \epsilon^*$. To summarize, we state the following theorem.

**Theorem 6.** *If $0 < \omega < T$, the extinction state undergoes a transcritical bifurcation at parameter $\epsilon = \epsilon^*$, as defined in equation (48). The bifurcating periodic orbit is biologically meaningful (positive) and stable, and the extinction equilibrium is unstable when $\epsilon < \epsilon^*$. When $\epsilon > \epsilon^*$, the extinction equilibrium is stable and the bifurcating periodic orbit loses biological relevance, becoming negative and unstable.*

### 6.2. *The case $\omega = T$*

To study the case where $\omega = T$, we will start with the original system (41)–(42) and make a few preliminary changes of variables and parameters. If we introduce the rescaled time $t \mapsto \frac{t}{T}$ and rescaled growth rate $\eta = rT$, the result is the system

$$\begin{aligned}\dot{x} &= \eta x\left(1 - \frac{x}{N}\right), \quad t \neq k \\ \Delta x &= -\epsilon x(k-1), \qquad t = k.\end{aligned} \tag{51}$$

Following Section 4, we define $y(t) = x(k-1)$ for $t \in (k-1,k]$. By definition of $y$, we see that $y(k) = x(k-1)$ and $y(k^+) = x(k)$. The finite-dimensional system associated to (51) takes the form

$$\begin{aligned}\dot{x} &= \eta x\left(1 - \frac{x}{N}\right), \quad t \neq k \\ \dot{y} &= 0, & t \neq k \\ \Delta x &= -\epsilon y, & t = k \\ \Delta y &= x - y, & t = k\end{aligned} \tag{52}$$

From here, one can readily compute the monodromy matrix associated to the linearization at the extinction equilibrium $(0,0)$. It is found to be

$$M_T = \begin{bmatrix} e^\eta & -\epsilon e^\eta \\ 1 & 0 \end{bmatrix}.$$

Notice that $M_T$ is rank two. This is in stark contrast to the case $\omega < T$, where the monodromy matrix was rank one. The Floquet multipliers also take a different form, being given by the pair

$$\mu_{1,2} = \frac{e^\eta}{2} \pm \sqrt{\frac{e^{2\eta}}{4} - \epsilon e^\eta}.$$

Consequently, when $\epsilon \geq e^\eta/4$, the eigenvalues become complex conjugate with modulus $|\mu_{1,2}| = \epsilon e^\eta$. Defining $\epsilon_{NS} = e^{-\eta}$, a Neimark-Sacker bifurcartion can therefore occur if $\epsilon_{NS} \geq e^\eta/4$. Note that the condition $\epsilon_{NS} \geq e^\eta/4$ is equivalent to $\eta \leq \log 2$. Biologically, this implies that a Neimark-Sacker bifurcation can only occur if the harvesting schedule is designed so that harvesting does not occur after small populations would double in size. The case $\eta = \log 2$ yields a 1:1 resonance.

Other situations can also be explored. For example, when $\epsilon \leq e^\eta/4$, both Floquet multipliers are real and nonnegative. One of the multipliers has unit modulus at any $\epsilon$ for which the equation

$$\pm\sqrt{\frac{e^{2\eta}}{4} - \epsilon e^\eta} = 1 - \frac{e^\eta}{2}$$

has a solution. The (unique) critical parameter where this occurs is is $\epsilon_F = 1 - e^{-\eta}$. When $\epsilon = \epsilon_F$, exactly one multiplier $\mu$ satisfies $\mu = 1$, while the other is strictly greater or less than one in modulus, unless it so happens that $\eta = \log 2$, resulting in the violation of a nondegeneracy condition. Notice also that it is always the case that $\epsilon_F \leq e^\eta/4$, with equality occuring when $\eta = \log 2$. Consequently, the potential fold bifurcation point always persists, independent of the sign of $\eta - \log 2$, which is in contrast with the Neimark-Sacker bifurcation point.

To conclude, there are three different cases that could be considered. If $\eta < \log 2$, then $\epsilon_{NS} < \epsilon_F$ with a potential Neimark-Sacker bifurcation at $\epsilon = \epsilon_{NS}$ and a potential fold bifurcation at $\epsilon_F$. If $\eta > \log 2$, a potential fold bifurcation occurs when $\epsilon = \epsilon_F$. The boundary point, $\eta = \log 2$, results in a 1:1 resonance at $\epsilon = \epsilon_F = \epsilon_{NS}$. The analysis of the resonant case will yield the best qualitative picture of the dynamics, so we will focus our attention there.

The linearization of (52) then takes the simple form

$$\dot{z} = \begin{bmatrix} \eta & 0 \\ 0 & 0 \end{bmatrix} z, \qquad t \neq k \tag{53}$$

$$\Delta z = \begin{bmatrix} 0 & -\epsilon \\ 1 & -1 \end{bmatrix} z, \quad t = k. \tag{54}$$

We will take $(\eta, \epsilon)$ as a bifurcation parameter. By the analysis earlier in this section, we know that the point $(\eta, \epsilon) = (\eta^*, \epsilon^*)$ with

$$(\eta^*, \epsilon^*) = \left(\log 2, \frac{1}{2}\right) \tag{55}$$

is a point at which the linearized system (53)–(54) has Floquet multipliers satisfying a 1:1 resonance condition. The matrix solution $v^X = [\, v^x \; v^y \,]$ of (53)–(54) is given for $t \in (0, 1]$ by

$$v^X(t) = \begin{bmatrix} 2^t & -2^{t-1} \\ 1 & 0 \end{bmatrix}.$$

Similar to the previous case where $\omega \neq T$, the quadratic terms in variables $(x, y)$ are solutions of the impulsive differential equations

$$\begin{aligned} \dot{v}^{\alpha\beta} &= \eta^* E_{11} v^{\alpha\beta} - e_1 \frac{2\eta^*}{N} v_x^\alpha v_x^\beta, \quad t \neq k, \; \alpha\beta \in \{xx, xy, yy\} \\ \Delta v^{\alpha\beta} &= (E_{21} - E_{22} - \epsilon^* E_{12}) v^{\alpha\beta}, \quad t = k, \; \alpha\beta \in \{xx, xy, yy\} \end{aligned} \tag{56}$$

with zero initial conditions. The solutions are easily computed for $t \in (0, 1]$ as

$$v^{xx}(t) = \begin{bmatrix} \frac{-2}{N} 2^t (2^t - 1) \\ 1 \end{bmatrix}, \; v^{xy}(t) = \begin{bmatrix} \frac{1}{N} 2^t (2^t - 1) \\ 1 \end{bmatrix}, \; v^{yy}(t) = \begin{bmatrix} \frac{-1}{2N} 2^t (2^t - 1) \\ 1 \end{bmatrix}.$$

Therefore, the stroboscopic map evaluated at the critical parameter satisfies

$$\begin{bmatrix} x \\ y \end{bmatrix} \mapsto \begin{bmatrix} 2 & -1 \\ 1 & 0 \end{bmatrix} \begin{bmatrix} x \\ y \end{bmatrix} + \begin{bmatrix} -\frac{2}{N}x^2 + \frac{2}{N}xy - \frac{1}{2N}y^2 \\ \frac{1}{2}x^2 + xy + \frac{1}{2}y^2 \end{bmatrix} + O^3(x,y) \tag{57}$$

Performing a linear transformation to send the linear part to Jordan canonical form results in the map

$$\begin{bmatrix} u_1 \\ u_2 \end{bmatrix} \mapsto \begin{bmatrix} 1 & 1 \\ 0 & 1 \end{bmatrix} \begin{bmatrix} u_1 \\ u_2 \end{bmatrix} + \begin{bmatrix} \frac{1}{2}\left(1 - \frac{1}{N}\right)u_1^2 + \frac{1}{N}u_1u_2 - \frac{9}{2N}u_2^2 \\ -\frac{1}{2N}u_1^2 - \frac{1}{N}u_1u_2 - \frac{9}{2N}u_2^2 \end{bmatrix} + O^3(u_1,u_2).$$

By [Kuznetsov, 2004] p. 433, the nondegeneracy conditions of bifurcation at 1:1 resonance are satisfied provided $N \neq 1$. In particular, it follows that the stroboscopic map associated to (52) can be approximated up to order 2 by a time-1 flow whose governing system of ordinary differential equations exhibits a Bogdanov-Takens bifurcation with normal form coefficient $s = \mathrm{sgn}(1-N)$. In particular, the following theorem holds.

**Theorem 7.** *If $\omega = T$ and $N \neq 1$, a bifurcation at 1:1 resonance occurs at the point $(\eta, \epsilon) = (\log 2, 1/2)$, where $\eta = rT$. In particular, transcritical bifurcations occur along the curve $(\eta, 1 - e^{-\eta})$ in a neighbourhood of $(\log 2, 1/2)$, and Neimark-Sacker bifurcations occur along the curve $(\eta, e^{-\eta})$ in a neighbourhood of $(\log 2, 1/2)$ in the half space defined by $\eta \leq \log 2$.*

To produce the bifurcation diagram, we must first write $(x,y) \mapsto S(x,y,\eta,\epsilon)$ as a Taylor expansion with respect to $(x,y)$. To compare, the map (57) is what one obtains when $(\eta,\epsilon) = (\log 2, 1/2)$, but we now wish to leave the parameters as arbitrary and (in principle) close to the critical parameters. Replacing $\eta^*$ with $\eta$ and $\epsilon^*$ with $\epsilon$ in the differential equations for $v^{\alpha\beta}$ in (56) results in the expansion

$$\begin{aligned} x &\mapsto e^{\eta}x - \epsilon e^{\eta}y - \frac{1}{N}e^{\eta}(e^{\eta}-1)x^2 + \frac{2}{N}\epsilon e^{\eta}(e^{\eta}-1)xy - \frac{1}{N}\epsilon^2 e^{\eta}(e^{\eta}-1)y^2 + O(||(x,y)||^3) \\ y &\mapsto x + \frac{1}{2}x^2 + xy + \frac{1}{2}y^2 + O(||(x,y)||^3). \end{aligned} \tag{58}$$

When $(\eta,\epsilon) = (\log 2, 1/2)$, the above is equivalent to (57). Next, we could obtain the bifurcation diagram analytically by computing the approximating flow for the above map. However, this is unnecessary for two reasons. First, we already know the location of the 1:1 resonance and the geometry of the Neimark-Sacker and fold curves, along with the sign of the asssociated Bogdanov-Takens normal form; they are given by Theorem 7 and the preceding discussion. Second, we can just as easily use bifurcation continuation software such as MATCONTM [Dhooge et. al, 2008] to produce the bifurcation diagram; see Figure 6.2.

### 6.2.1. *Discussion of the bifurcation diagram*

Referring to Figure 6.2, we will describe the decomposition of the parameter space close to the 1:1 resonance point. We will say that a fixed point or periodic orbit is conditionally stable if one of its multipliers lies within the complex unit disc, while the other lies outside. Also, such a point is oscillatory if its eigenvalues have nonzero imaginary part.

The dynamics in region A and B differ depending on the normal form coefficient $s = \mathrm{sign}(1-N)$. If $s = -1$, region A contains a time-varying closed curve that is stable and invariant under the impulsive dynamics, oscillating from positive to negative in sign, while the extinction equilibrium is conditionally stable and oscillatory. Upon passing into region B, the invariant closed curve is destroyed by a Neimark-Sacker bifurcation. If $s = 1$, region A contains only the conditionally stable oscillatory extinction equilibrium, while passing into region B produces an unstable time-varying curve through a Neimark-Sacker bifurcation. In both cases, the extinction equilibrium is stable and oscillatory in region B.

Passing into region C, the eigenvalues become real and the trajectories are biologically meaningful. Near the boundary to region D, there is a negative periodic orbit that is conditionally stable. A transcritical bifurcation occurs when crossing the boundary between region C and D, with the result being a stable, positive periodic orbit. In region D, the extinction equilibrium is conditionally stable. The periodic orbit becomes unstable in region E through some bifurcation that is not detectable because it is nonlocal and the second-order truncation of (57) does not accurately capture such nonlocal effects. The extinction

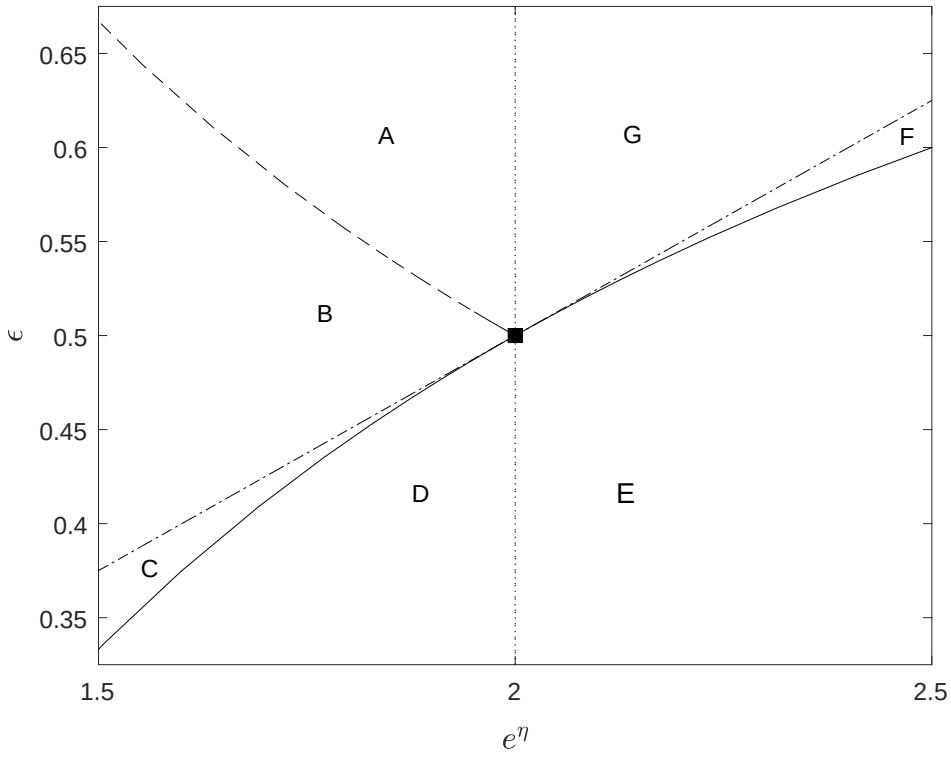


Fig. 2. The bifurcation diagram for the 1:1 resonance case of the logistic model with census delay and $\omega = T$. Fold bifurcations occur along the solid line ($\epsilon = 1 - e^{-\eta}$), while Neimark-Sacker bifurcations occur along the dashed line ($\epsilon = e^{-\eta}$). Their intersection at the black square is a 1:1 resonance point. The vetical dotted line delineates a stability-instability boundary associated to the fold bifurcation curve, while the oblique dash-dot line ($\epsilon = e^{\eta}/4$) indicates where the multipliers of the extinction equilibrium pass from real to complex-conjugate. Note that only the bifurcation curves described in Theorem 7 were searched for in MATCONTM; the other curves appearing in the diagram were manually added, since they do not correspond to true bifurcation curves.

equilibrium maintains its conditional stability in region E. Passing into region F, the final transcritical bifurcation takes place, with the periodic orbit becoming negative and conditionally stable and the extinction equilibrium becoming unstable. Passing into region G, the extinction equilibrium becomes oscillatory.

To conclude, the region of parameter space where small positive trajectories remain biologically relevant is given by the union of regions C,D,E and F. The only local bifurcations at the extinction equilibrium in this region are transcritical bifurcations. Due to this observation and the analysis of Section 6.1, we can make the following corollary.

**Corollary 6.1.** *Given a census $\omega \in (0, T]$, define $[\omega] = \omega$ if $\omega < T$ and $[\omega] = 0$ if $\omega = T$. The logistic model with delayed census harvesting* (41)–(42) *undergoes a transcritical bifurcation at the extinction equilibrium with critical parameter $\epsilon^* = e^{r[\omega]}(1-e^{-rT})$. The nonnegative orbit structure is identical to the one described in Theorem 6 and if $rT \leq \log 2$, the stability conclusions are also valid.*

## 7. Conclusions

Section 2 reviewed some elementary properties of the stroboscopic map associated to an impulsive differential equation. It was shown that the stroboscopic map is smooth (Proposition 1), and Theorem 2 demonstrated that the Taylor coefficients of the stroboscopic map at a given periodic orbit (identified with a fixed point) can be computed up to a given order by solving a tiered system of linear impulsive differntial equations. These results are applicable even if the period of the impulsive system or the impulse times themselves vary with the parameter. In Section 3, we outlined the Lyapunov-Schmidt reduction (Section 3.1) and center manifold reduction (Section 3.2) methods as they apply to the stroboscopic map. Section

4 explained how a class of impulsive delay differential equations can be converted to a finite-dimensional system of impulsive systems without delays, so that the aforementioned methods of bifurcation theory are applicable.

Two examples were studied to illustrate the reduction methods. The SIR model with impulsive treatment at irregular times was considered in Section 5. Both the Lyapunov-Schmidt reduction and the center manifold reduction were used to prove the existence of a transcritical bifurcation, thereby comparing both methods. Next, a logistic equation with delayed impulsive harvesting was considered in Section 6. Transforming to the higher-dimensional system without delays according to the methods of Section 4, it was shown that for most cases, a transcritical bifurcation occurs. However, in the situation where the delay is perfectly synchronized with the harvesting (Section 6.2), Neimark-Sacker bifurcations are possible. In particular, there is a 1:1 resonance point nearby which the system exhibits both transcritical and Neimark-Sacker bifurcations (Theorem 7). The bifurcation diagram was given and the orbit structure and stability was characterized in the seven regions of parameter space of interest near the resonance point.

## References


M. Bachar, J.G. Raimann and P. Kotanko [2016] *Impulsive mathematical modeling of ascorbic acid metabolism in healthy subjects*, J. Theoretical Biology, 392, 35–47

Bainov, D.D. and Simeonov, P.S. [1993] *Impulsive Differential Equations: Periodic Solutions and Applications.* (Longman Scientific & Technical)

K.E.M. Church and R.J. Smith? [2016] *Comparing malaria surveillance with periodic spraying in the presence of insecticide-resistant mosquitoes: should we spray regularly or based on human infections?*, Math. Biosci., 276, 145–163.

A. Dhooge, W. Govaerts, Y.A. Kuznetsov, H.G.E. Meijer & B. Sautois [2008] *New features of the software MatCont for bifurcation analysis of dynamical systems*, MCMDS, 14(2), 147–175.

X. Liu and P. Stechlinski [2012] *Infectious disease models with time-varying parameters and general nonlinear incidence rate*, Applied Mathematical Modelling 36, 1974–1994.

X. Liu and Q. Wang [2008] *Impulsive Stabilization of High-Order Hopfield-Type Neural Networks With Time-Varying Delays*, IEEE Transactions on Neural Networks, 19(1), 71–79.

Y. A. Kuznetsov [2004] *Elements of Applied Bifurcation Theory*, Third edition (Springer-Verlag New York)

L.H. Loomis and S. Sternberg [1968] *Advanced Calculus* (Addison-Wesley Publishing Company)

L. Pang, L. Shen and Z. Zhao [2016] *Mathematical Modelling and Analysis of the Tumor Treatment Regimens with Pulsed Immunotherapy and Chemotherapy*, Comput. Math. Methods Med.

C. Rozins and T. Day [2017] *The industrialization of farming may be driving virulence evolution*, Evolutionary Applications, 10(2), 189–198

S. Wiggins [2003] *Introduction to Applied Nonlinear Dynamical Systems and Chaos* (Springer-Verlag, New York).

Y. Xia [2011] *Global analysis of an impulsive delayed Lotka-Volterra competition system*, Commun Nonlinear Sci Simulat, 16, 1597–1616

Y. Xie, L. Wang, Q Deng and Z. Wu [2017] *The dynamics of an impulsive predator–prey model with communicable disease in the prey species only*, Applied Mathematics and Computation, 292, 320–335

H. Yu, S. Zhong, R.P. Agarwal and L Xiong [2010] *Species permanence and dynamical behavior analysis of an impulsively controlled ecological system with distributed time delay*, Computers and Mathematics with Applications, 9, 3824–3835

M. Zhao, X. Wang, H. Yu and J. Zhun [2012] *Dynamics of an ecological model with impulsive control strategy and distributed time delay*, Mathematics and Computers in Simulation, 82, 1432–1444

X. Zhang, Z. Shuai and K. Wang [2003] *Optimal impulsive harvesting policy for single population* Nonlinear Analysis: Real World Applications, 4(4), 639–651

J. Zhou, L. Xiang and Z. Liu [2007] *Synchronization in complex delayed dynamical networks with impulsive effects*, Physica A: Statistical Mechanics and its Applications, 384(2), 684–292.